2nd IAEA Technical Meeting on Collisional-Radiative properties of Tungsten and Hydrogen in Edge Plasma of Fusion Devices, 28 Nov. - 2 Dec. 2023, Vienna International Centre

ASIPP

Tungsten density and influx evaluations based on the latest atomic data in EAST plasma

ZHANG Ling [1*], ZHANG Fengling [1,2], MITNIK Darío [3,1], ZHANG Wenmin [1,2], CHENG Yunxin [1], HU Ailan [1], MORITA Shigeru [4,1], CAO Yiming [1,5], MA Jiuyang [1,2], LI Zhengwei [1,5], JIE Yinxian [1], LIU Haiqing [1]

[1] *Institute of plasma physics, Chinese Academy of Sciences, Hefei 230026, China*

[2] *University of Science and Technology of China, Hefei 230026, China*

[3] *Instituto de Astronomía y Física del Espacio（IAFE）, Buenos Aires 1428, Argentina*

[4] *National Institute for Fusion Science, Toki 509-5292, Gifu, Japan*

[5] *Anhui University, Hefei 230601, China*

Acknowledgement: National Key Research and Development Program of China (2022YFE03180400, 2019YFE030403, 2018YFE0311100, 2018YFE0303104 and 2022YFE03020004), National Natural Science Foundation of China (Grant Nos. 12322512, 11905146, 11975273 and 12075283), and Chinese Academy of Sciences President's International Fellowship Initiative (PIFI) (Grant No. 2020VMA0001).

***Email:** zhangling@ipp.ac.cn **29 Nov. 2023**

Outline

- Background & Motivation
- Tungsten spectroscopic diagnostics
- Tungsten line identification and density profiles
- Tungsten influx evaluation: S/XB calculation
- Summary & Future work

Outline

ASIPP

- Background & Motivation
- Tungsten spectroscopic diagnostics
- Tungsten line identification and density profiles
- Tungsten influx evaluation: S/XB calculation
- Summary & Future work

EAST PFCs upgrade

ASIPP

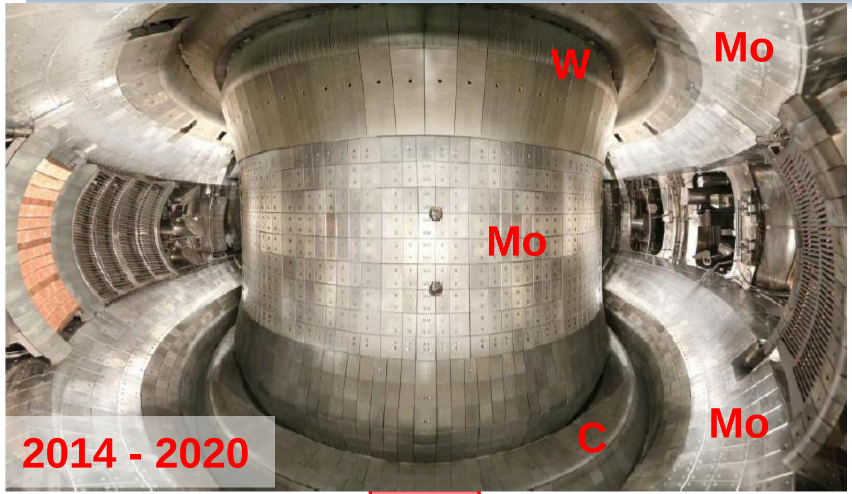

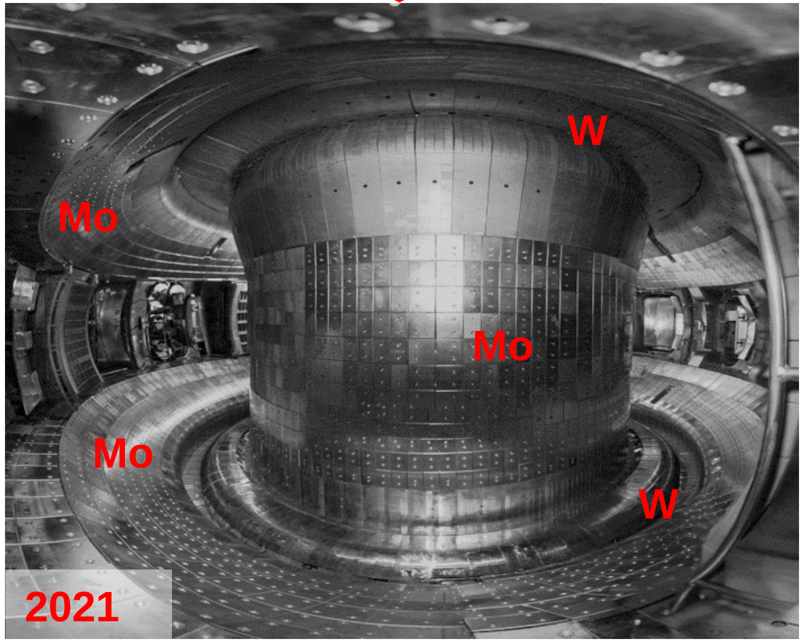

Full tungsten divertor from May 2021

First Wall: TZM (Titanium-Zirconium-Molybdenum) alloy

Upper divertor: ITER-like W/Cu monoblock

Lower divertor: W/Cu monoblock

Upper W-divertor

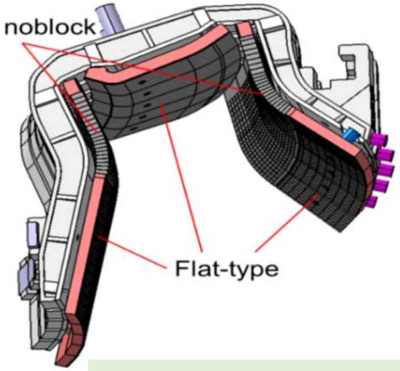

Lower W-divertor

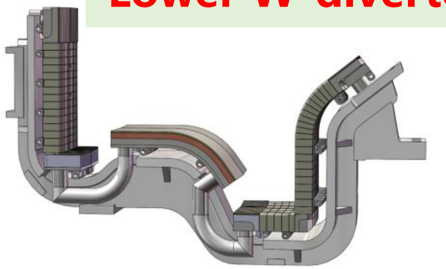

2018 Guard limiters antenna (LHW): C → W
2022/3 Main limiter: C → W
2022/5 Main limiter: W → Mo
LHW / ICRF antenna: Cu / Fe

Guider limiter for LHW antenna

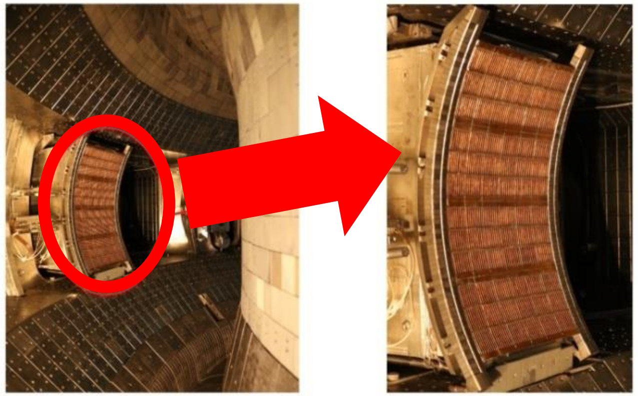

Intrinsic & extrinsic impurities;
He, Li, (B), C, N, O, (Ne), (Si), (Ar), Fe, Cu, Mo, W…

Requirement of tungsten spectroscopy measurement

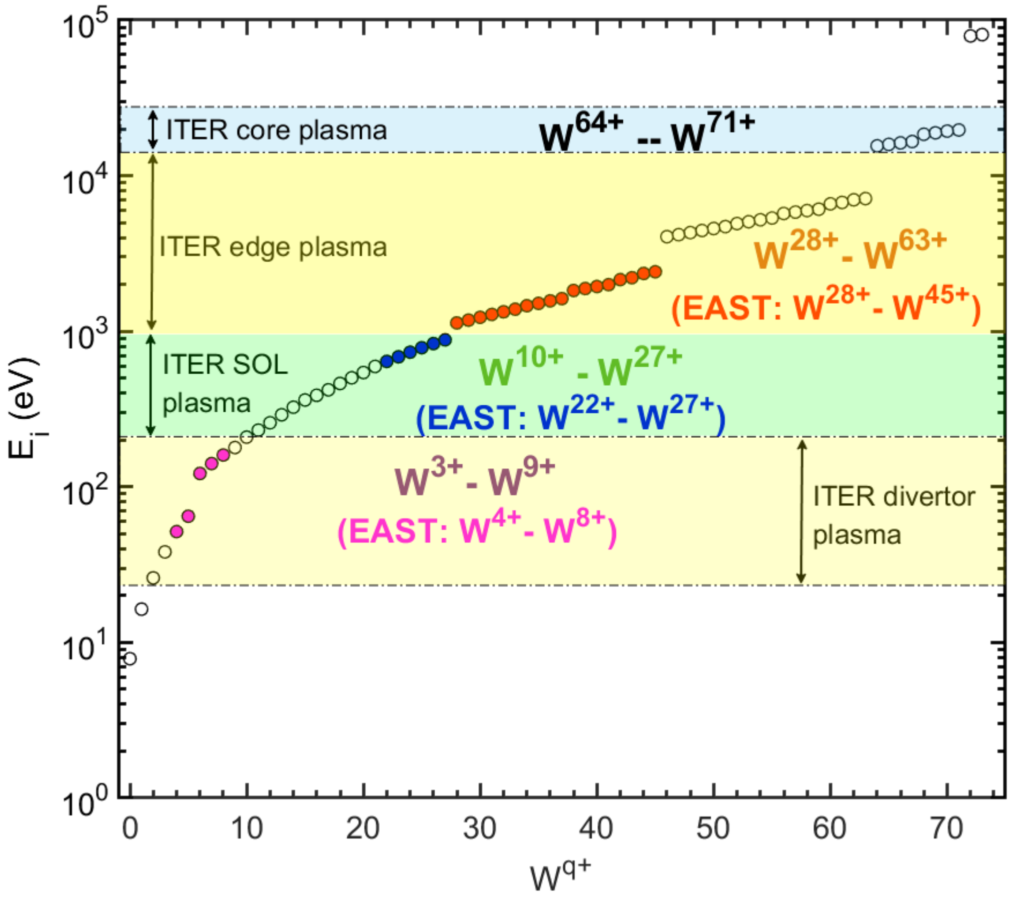

- Observation of **W^{0}-W^{28+} ions existing in Div.-SOL-pedestal** of ITER or EAST plasma is crucial important for tungsten production, penetration and edge transport study.
- **M1 forbidden transition of W^{7+} - W^{28+}** have been observed in visible wavelength range in Shanghai EBIT, CoBIT and LHD.
- **Quantitative study**
  - Lack of **W influx** calculation except W^{0} (4009 Å)
  - **W^{24+}-W^{45+} ions and its density profiles** are observed in EAST

EAST	Capability	Diagnostic
Divertor	Upper & lower div. W source – **W^{0} (4009Å)**	**Space-resolved VIS**
	Upper div. W source (**2D**) – **W^{0}** (4009Å, 4295Å, 5053Å) – **W^{1+}** (4218Å, 4348Å)	**Space-resolved VIS (2D)**
SOL (ρ=1.0-1.05)	W influx (**W^{3+}-W^{6+}: 500-1500Å**)	**VUV survey**
	W influx (**W^{3+}-W^{6+}: 200-500Å**)	**EUV survey**
Pedestal / edge	W influx & density – **W^{7+}-W^{20+}: 150-260Å**	**EUV survey**
Bulk plasma (ρ≤0.7)	W density profile – **W^{24+}-W^{45+}: 15-140Å**	**Space-resolved EUV**

Outline

ASIPP

- Background & Motivation
- Tungsten spectroscopic diagnostics
- Tungsten line identification and density profiles
- Tungsten influx evaluation: S/XB calculation
- Summary & Future work

Fast-time-response EUV spectrometers (5ms/frame)

Since 2021

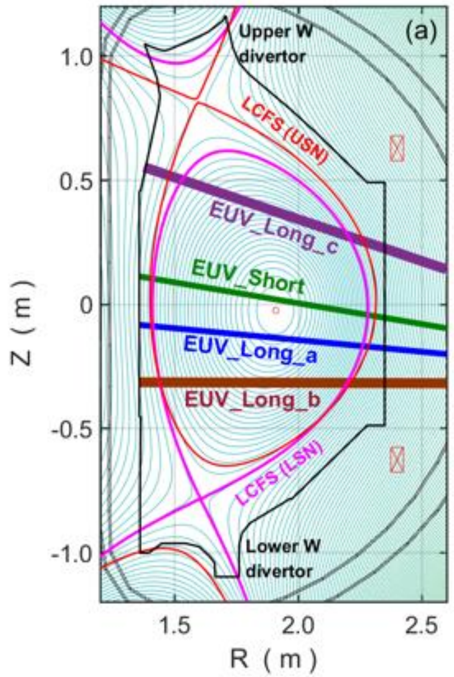

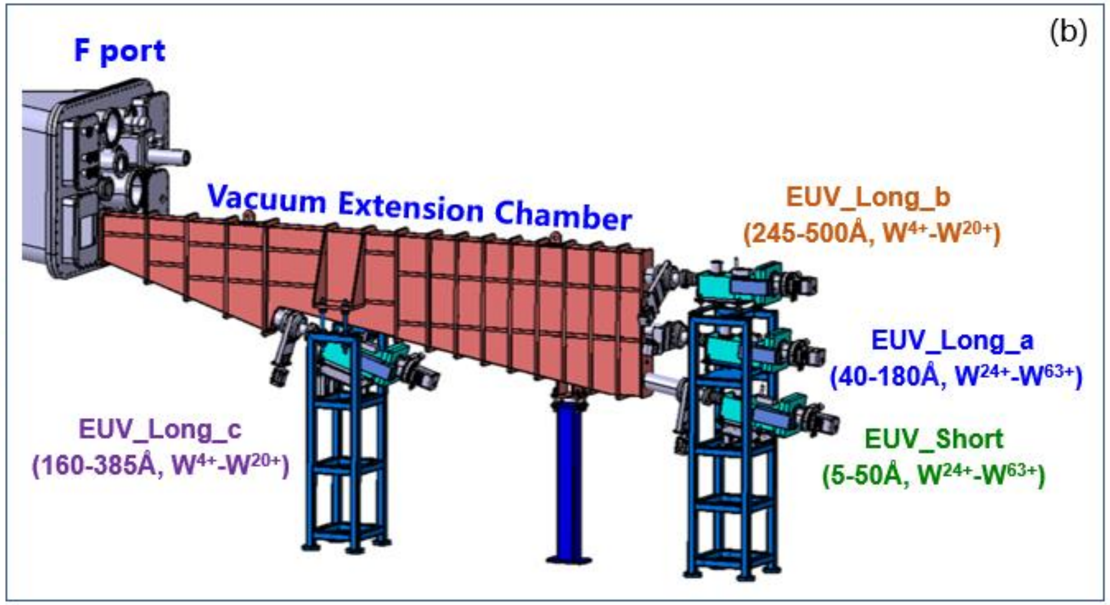

Status prior to 2021:
only EUV_Short and EUV_Long_a **(scanning λ)**

Grazing Incidence flat-field spectrometer

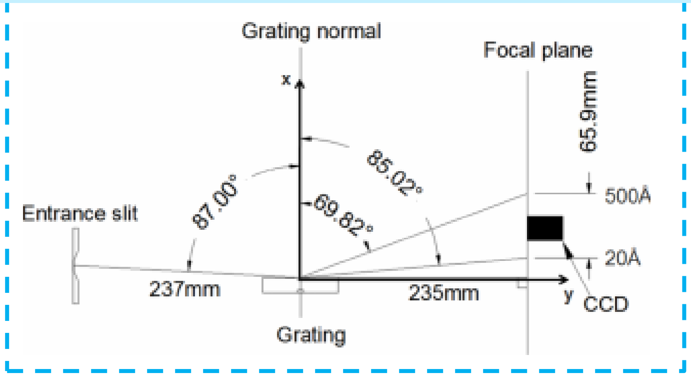

		EUV_Short	EUV_Long_a	EUV_Long_c	EUV_Long_b
λ	Capability	5-138 Å	20-500 Å		
	Operation	5-50 Å	40-180 Å	160-385 Å	245-500 Å
Ions		He^{+}, Li^{+}-Li^{2+}, C^{2+}-C^{5+}, O^{2+}-O^{7+}, Ne^{+}-Ne^{9+}, Si^{4+}-Si^{11+}, Ar^{9+}-Ar^{15+}, Fe^{4+}-Fe^{23+}, Cu^{9+}-Cu^{26+}, Mo^{4+}-Mo^{31+}, **W^{3+}-W^{63+}**, …			

L. Zhang Rev. Sci. Instrum. 86 (2015)123509

Z. Xu Nucl. Instrum. Meth. A1010 (2021) 165545

- **Spectrometers**
  - **Entrance slit: 30μm**
  - **Gratings: 2400 g/mm (Short)**
    1200 g/mm (Long)
- **Detector: Andor BO920U**
  - **1024 x 256, 26μm/pixel**
  - **1024 (H) spectral measurement**
  - **256 (V) full binning: 5ms/frame**
- **Pulse motor for wavelength scan**
- **Laser light for optical alignment**
- **Turbo-molecular pump for vacuum**

Space-resolved EUV spectrometers ($\rho\leq0.7$)

ASIPP

Since 2021

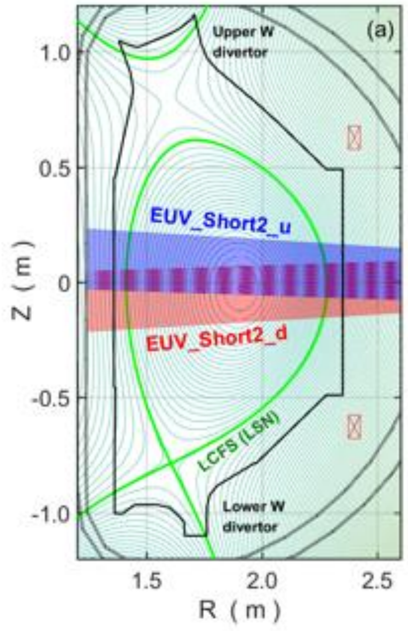

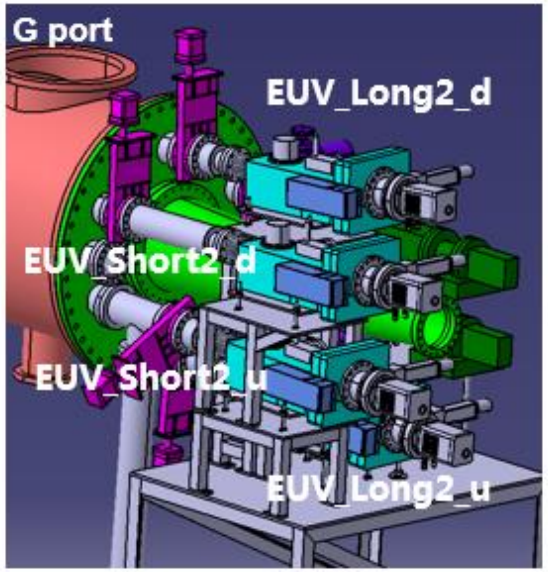

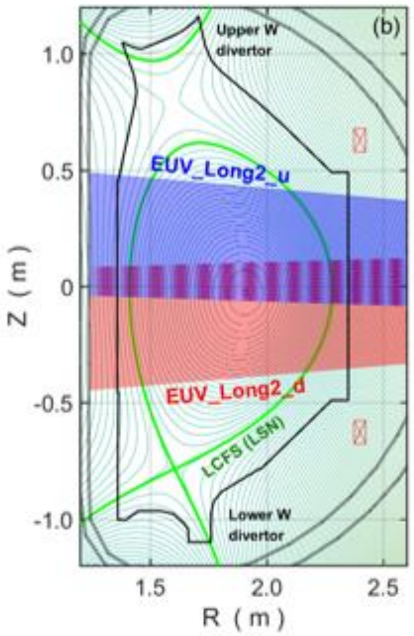

Status prior to 2021:
only EUV_Long2_U **(scanning Z)**

- **Spectrometers**
  - **Entrance slit: 100μm**
  - **Space-resolved slit: 1mm**
  - **Gratings: 2400 g/mm (Short2)**
    1200 g/mm (Long2)
- **Detector (Long2)**
  - **Andor BO920U:1024 x 256, 26μm/pix**
  - **256 (H) spectral measurement**
  - **1048 (V) space-resolved measurement**
- **Detector (Short2)**
  - **Andor Marana-X: 2048 x 2048, 6.5μm/pix**
  - **2048 (H) spectral measurement**
  - **2048 (V) space-resolved measurement**

	λ range	Temporal Reso.	Spatial Reso.	Viewing range	Detector
EUV_Short2	5-130 Å	15 ms/frame	≥0.3 cm	±25 cm	CMOS
EUV_Long2	30-520 Å	200 ms/frame	≥0.8 cm	±45 cm	CCD
Ions ($\rho\leq0.7$)	W^{24+}-W^{63+}, Mo^{24+}-Mo^{31+}, Cu^{19+}-Cu^{26+}, Fe^{18+}-Fe^{23+}…				

✓ L. Zhang ***Nucl. Instrum. Meth. A*** 916 (2019) 169
✓ Y.X. Cheng ***Rev. Sci. Instrum.*** 93 (2022)123501

High spectral resolution is necessary for tungsten spectra observation and identification

ASIPP

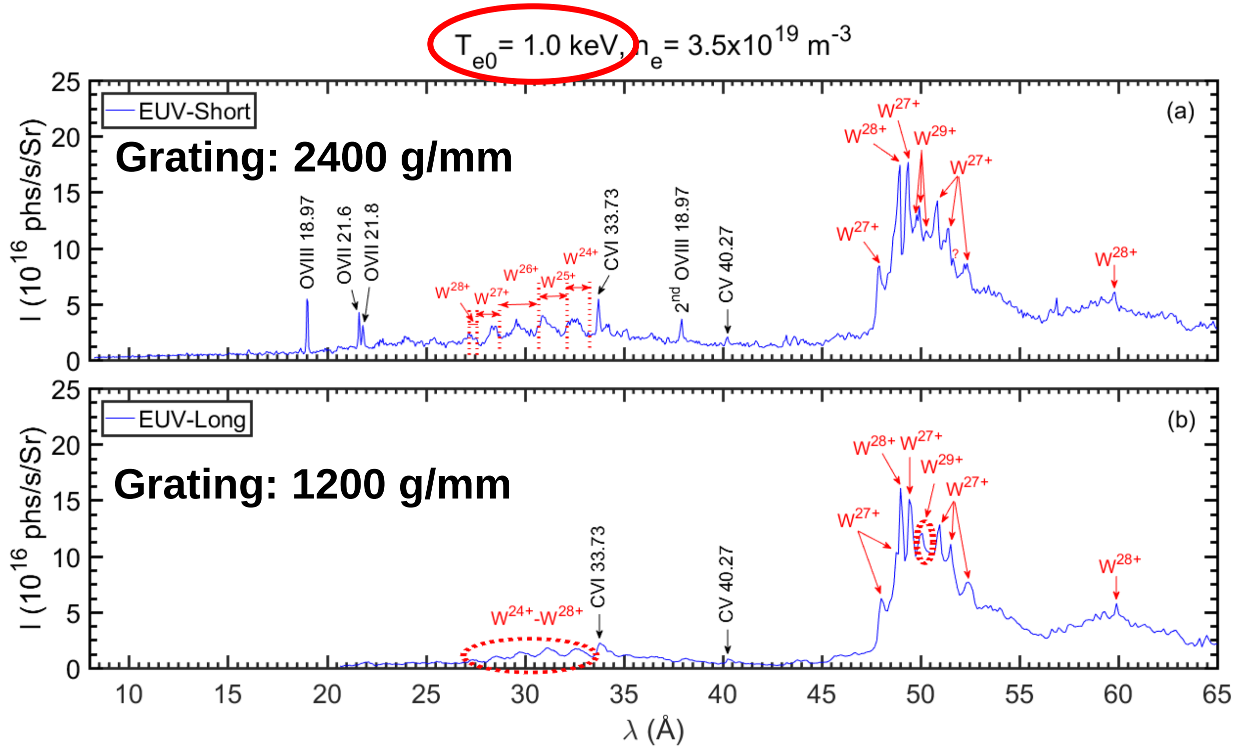

W-UTA: tungsten unresolved transition array

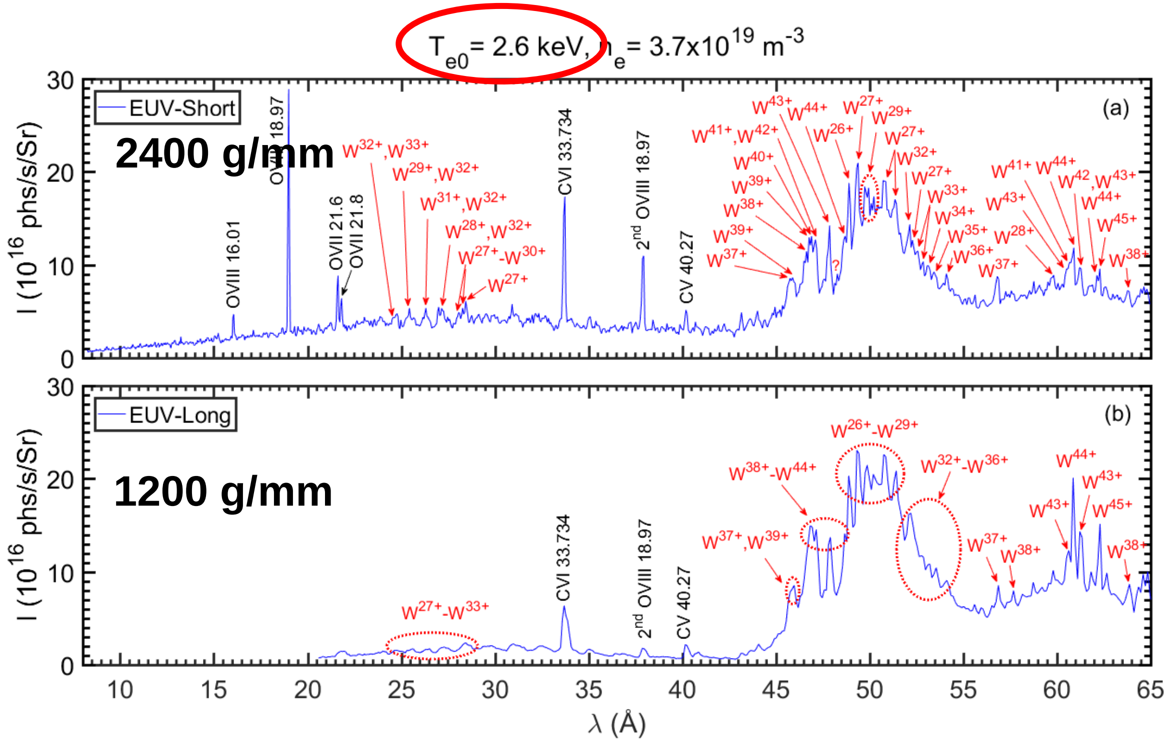

- Also high accurate wavelength measurement
  $\Delta\lambda=|\lambda_{obs}-\lambda_{sta}|\leq0.03$Å for EUV_Short; $\Delta\lambda=|\lambda_{obs}-\lambda_{sta}|\leq0.08$Å for EUV_Long
- Higher spectral resolution at 8-65 Å for EUV_short with 2400g/mm grating
- Structure and ion composition of W-UTA changes dramatically with T_e

Z Xu ***Nucl. Instrum. Meth. A*** 1010 (2021) 165545

Observation of W-UTA with finer structure by using CMOS detector with smaller pixel size

ASIPP

W-UTA: tungsten unresolved transition array

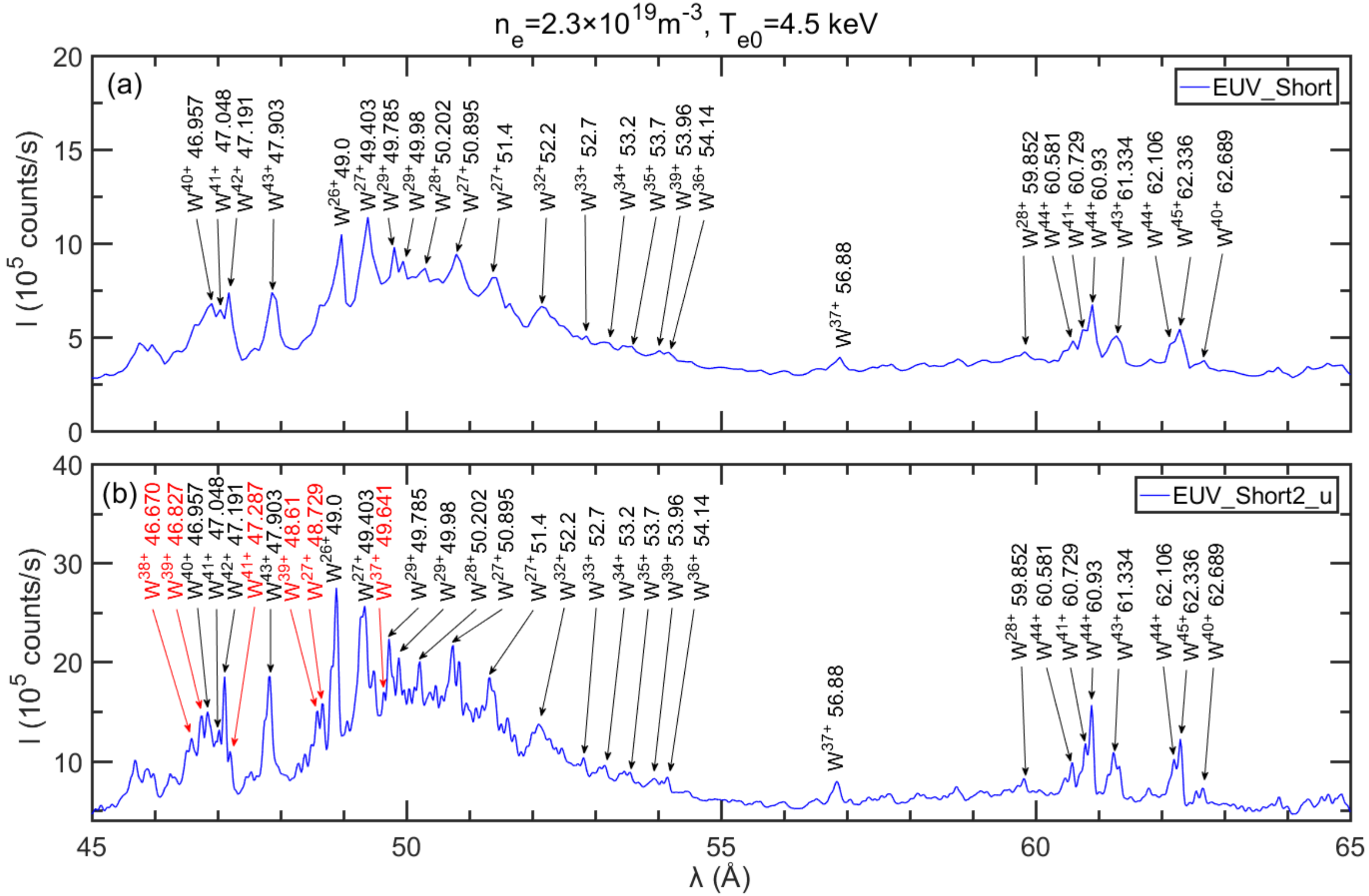

CCD detector (26 μm/pixel)

CMOS detector (6.5 μm/pixel)

Y.X. Cheng ***Rev. Sci. Instrum.*** 93 (2022)123501

Capability of fast time history observation of W ion distribution allowing W transport study during low-frequency sawtooth activity

ASIPP

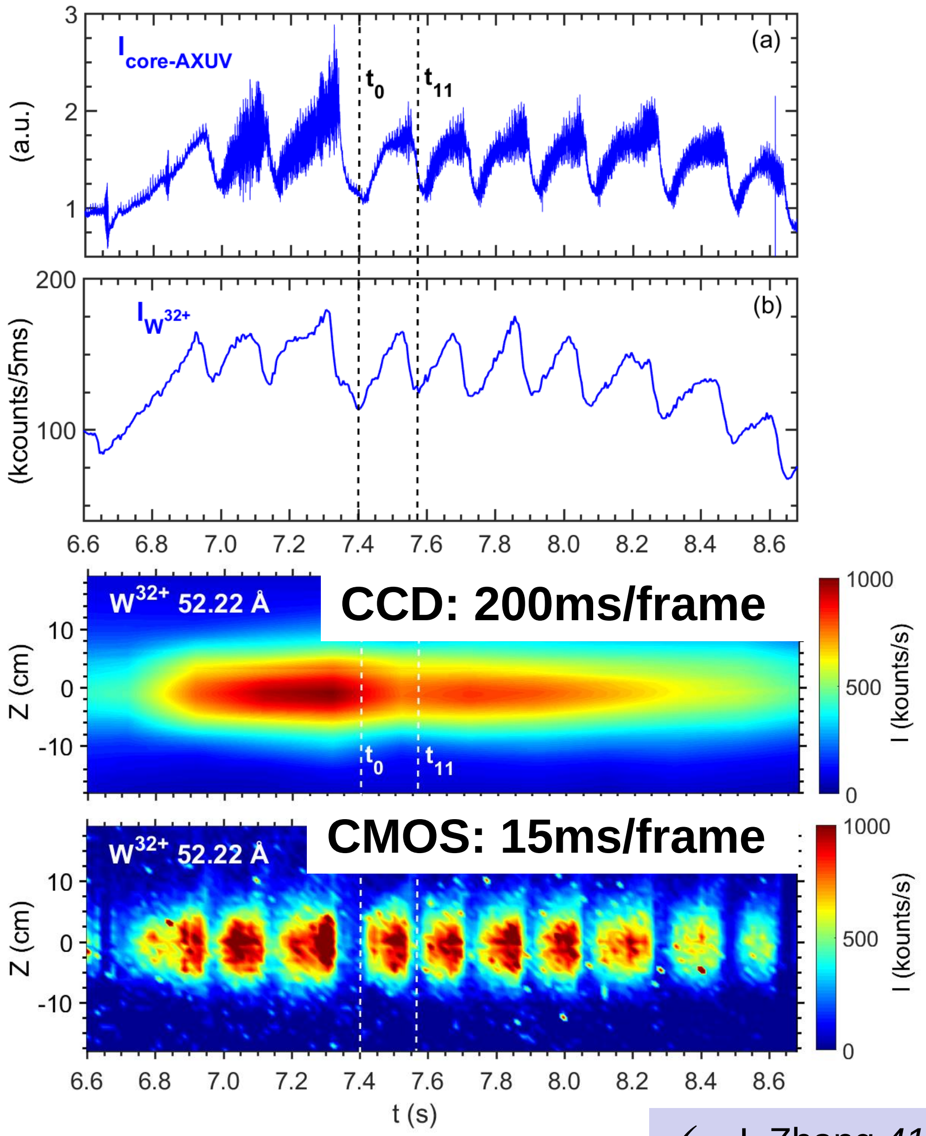

W^{32+}

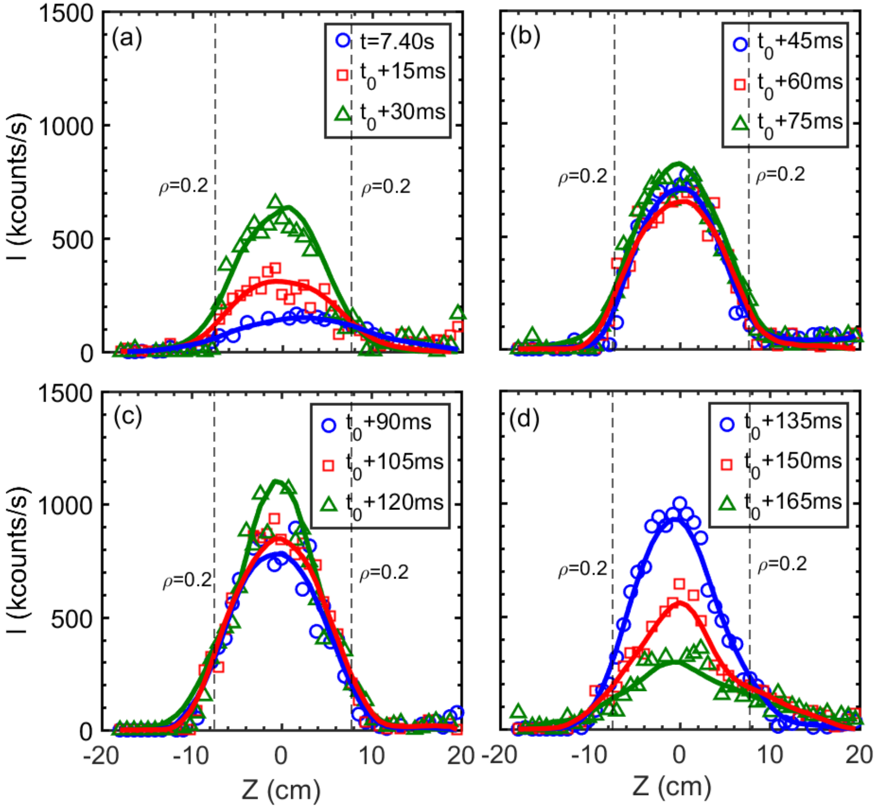

- Temporal evolution of W^{32+} profile during one sawtooth cycle

✓ L Zhang *41st ITPA-DG* 2022

✓ Y.X. Cheng ***Rev. Sci. Instrum.*** 93 (2022)123501

Full profile measurement extended to W ions with lower change state after upgrade of space-resolved EUV spectrometers

ASIPP

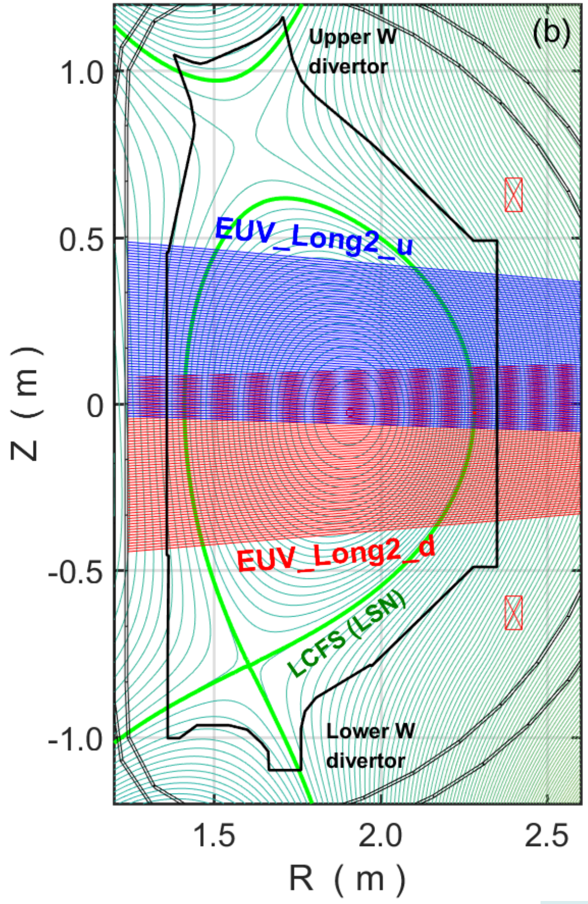

H-mode vs. L-mode (RF)

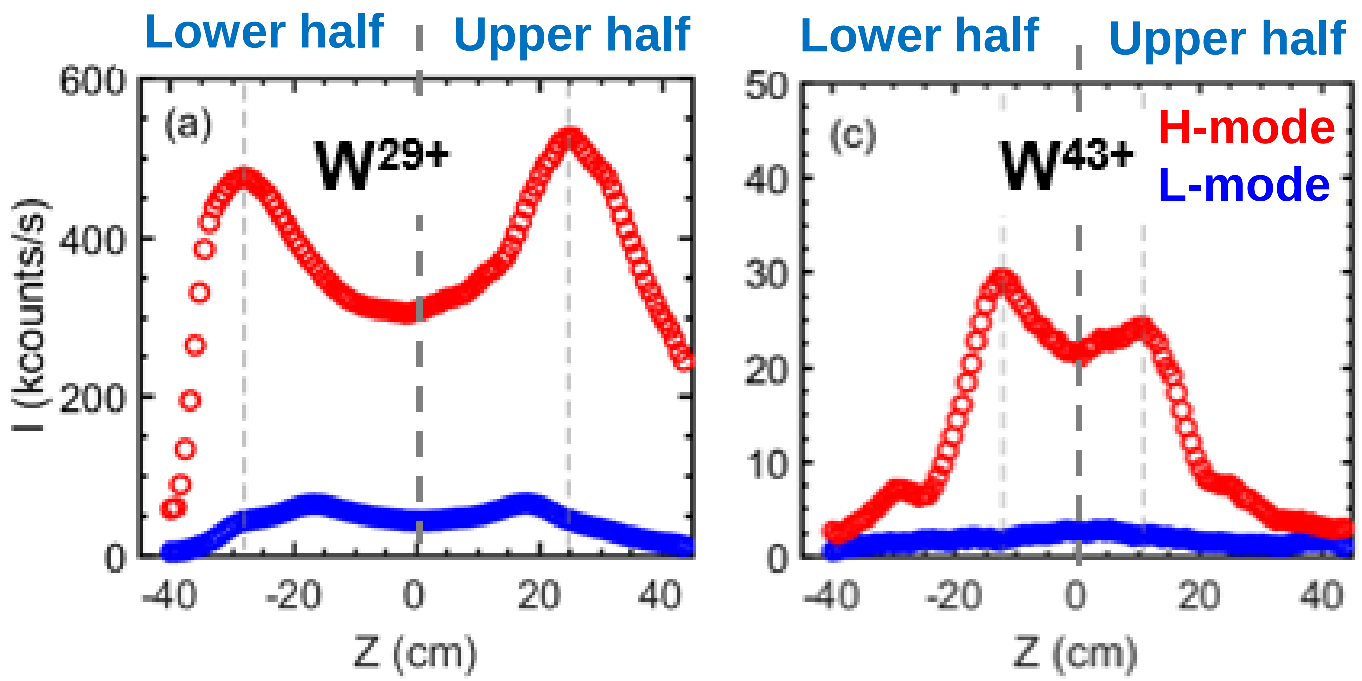

- Shell-like distribution in RF-heated H-mode, but not for tungsten accumulation case
- Radial (vertical) profiles of line intensity will help to line identification

Outline

ASIPP

- Background & Motivation
- Tungsten spectroscopic diagnostics
- Tungsten line identification and density profiles
- Tungsten influx evaluation: S/XB calculation
- Summary & Future work

Isolated W^{40+}-W^{45+} lines are essential for quantitative analysis of radial profile of W ion density

ASIPP

Line identification in 43-137Å at T_{e0}~3.0 keV

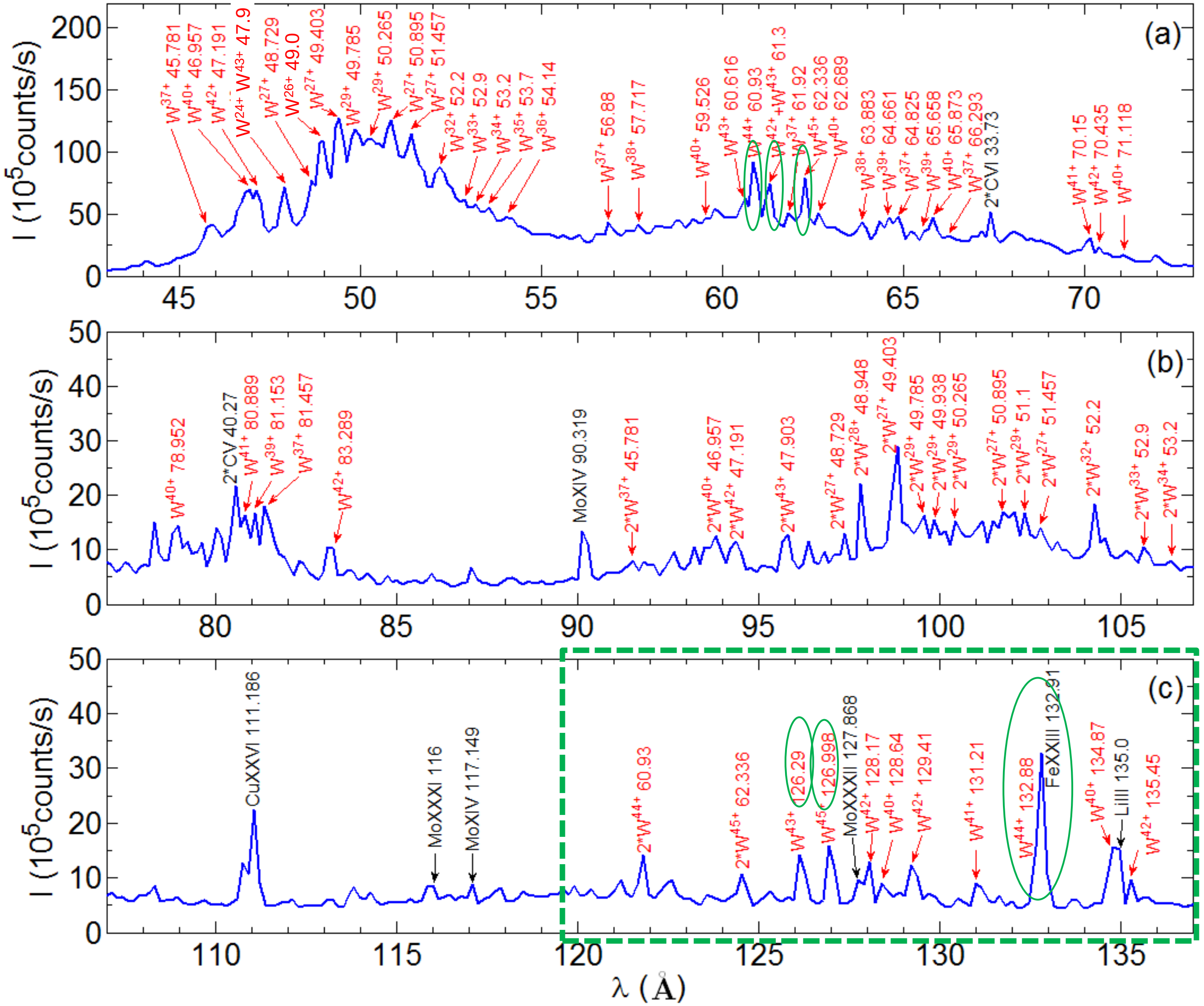

- W lines are identified based on NIST database.
- W^{43+} - W^{45+} lines with strong intensity are identified from W-UTA at ~60Å.
- Isolated W^{40+} - W^{45+} lines with weak intensity is identified at longer wavelength range of 120-140Å.

Important lines for quantitative analysis

- **W^{43+} (E_i=2.210keV)**
  $4s^24p$-$4s$ (61.334, 126.29Å)
- **W^{44+} (E_i=2.354keV)**
  $4s4p$-$4s$ (60.93, 132.88Å)
- **W^{45+} (E_i=2.414keV)**
  $4p$-$4s$ (62.336, 126.998Å)

✓L Zhang Nucl. Instrum. Meth. A 916 (2019) 169

Traditional method based on EFIT equilibrium and Abel inversion for analyzing radial profiles of impurity ion density

ASIPP

- Impurity density profile is analyzed from vertical profile of impurity line intensity

$$I^{W^{q+}}(Z) = \int n^{W^{q+}}(Z,r) PEC^{W^{q+}}(Z,r) n_e(Z,r) dr$$

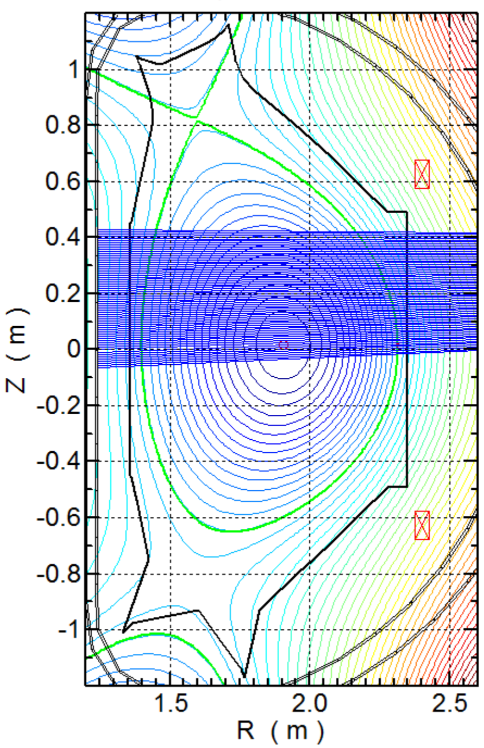

Vertical profile: $I^{W^{q+}}(Z)$

⇓ EFIT equilibrium, Abel Inversion

Local emissivity profile: $\varepsilon^{W^{q+}}(r)$

⇓ $T_e(r)$, $n_e(r)$, **PEC(T_e,n_e)**

Density profile: $n^{W^{q+}}(r)$

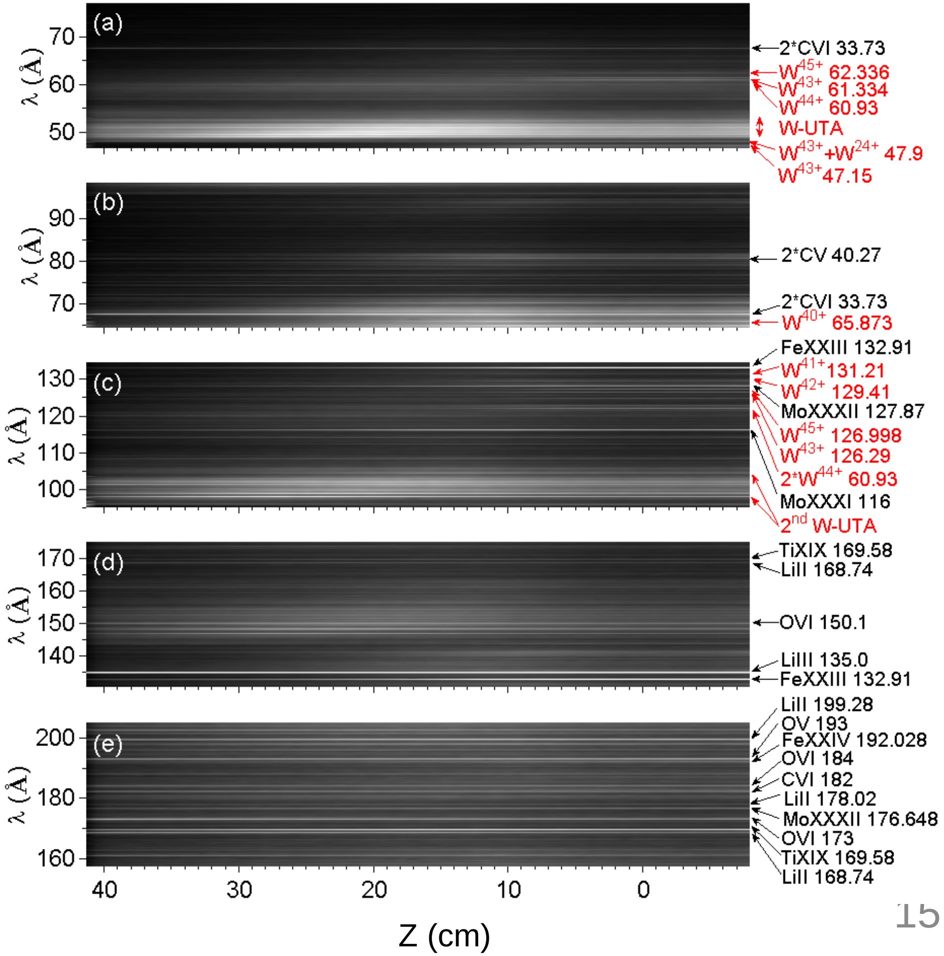

Radial profiles of local emissivity and tungsten ion density

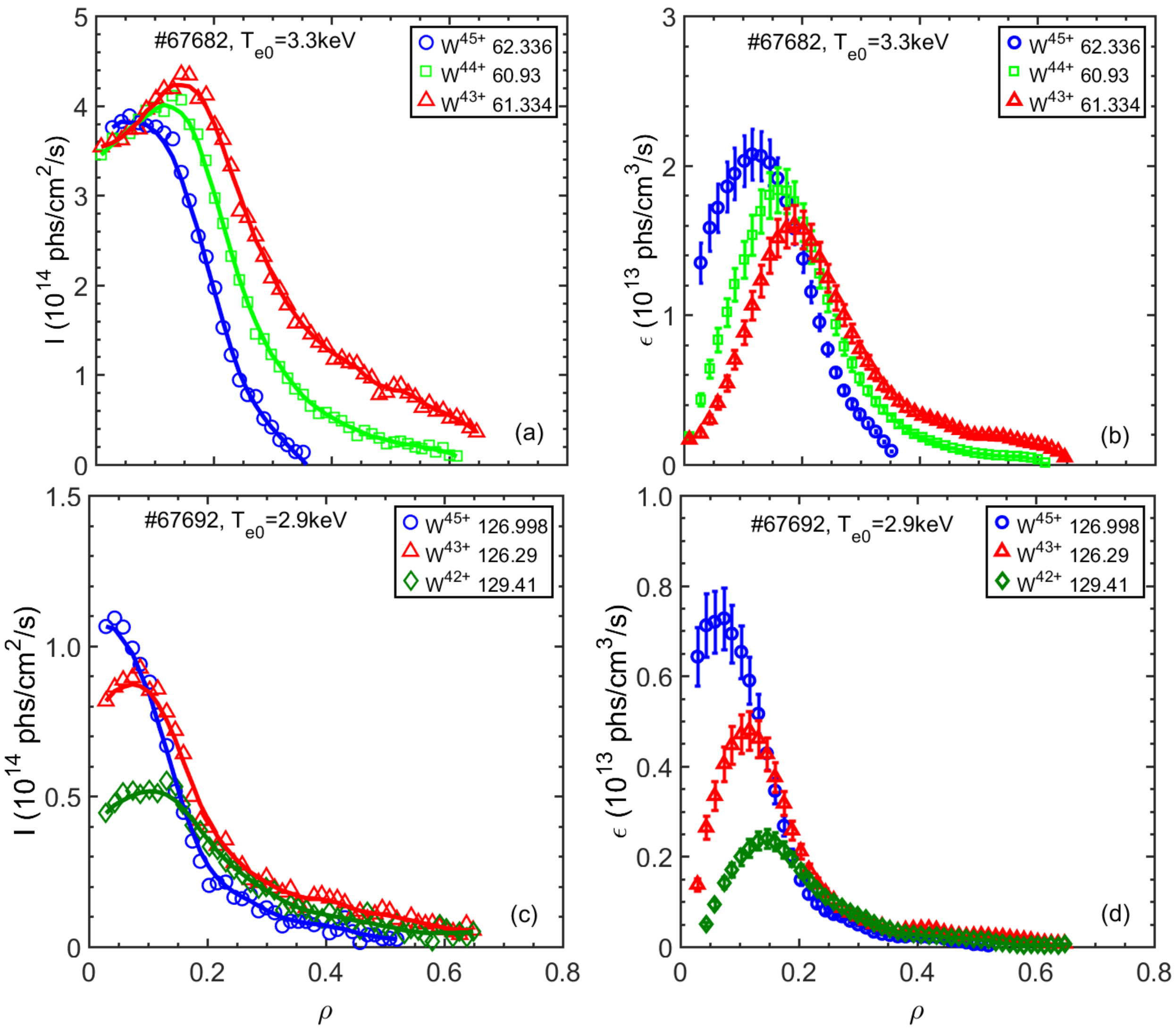

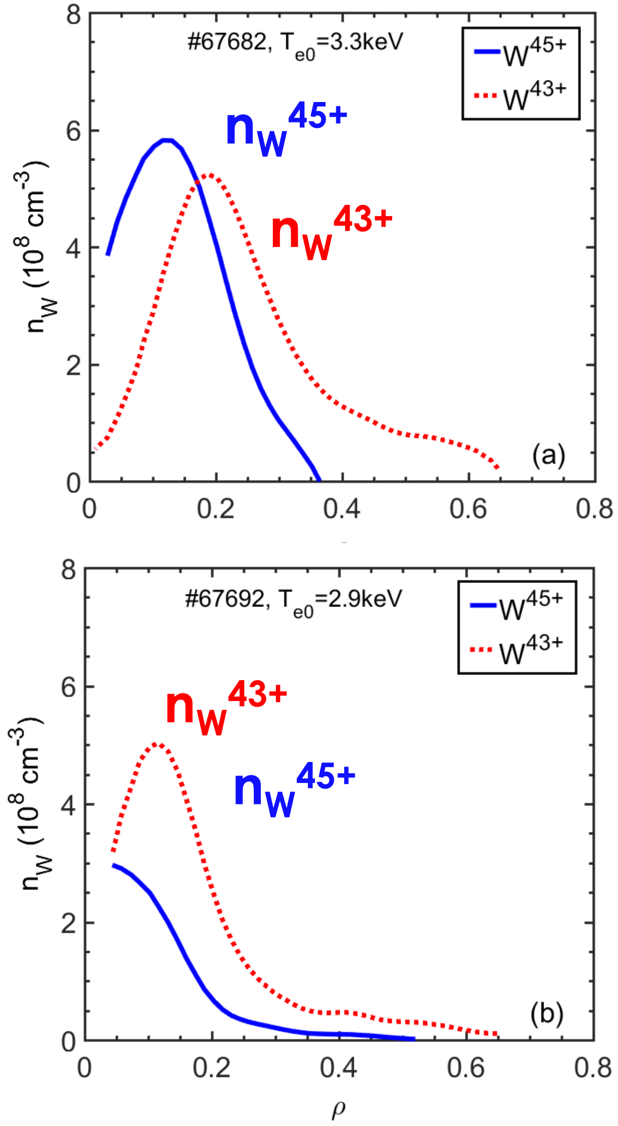

✓ L Zhang et al Nucl. Instrum. Meth. A 916 (2019) 169

Observation and identification of W ions with low ionization stage in a discharge with tungsten sputtering (T_{e0}~3.0keV)

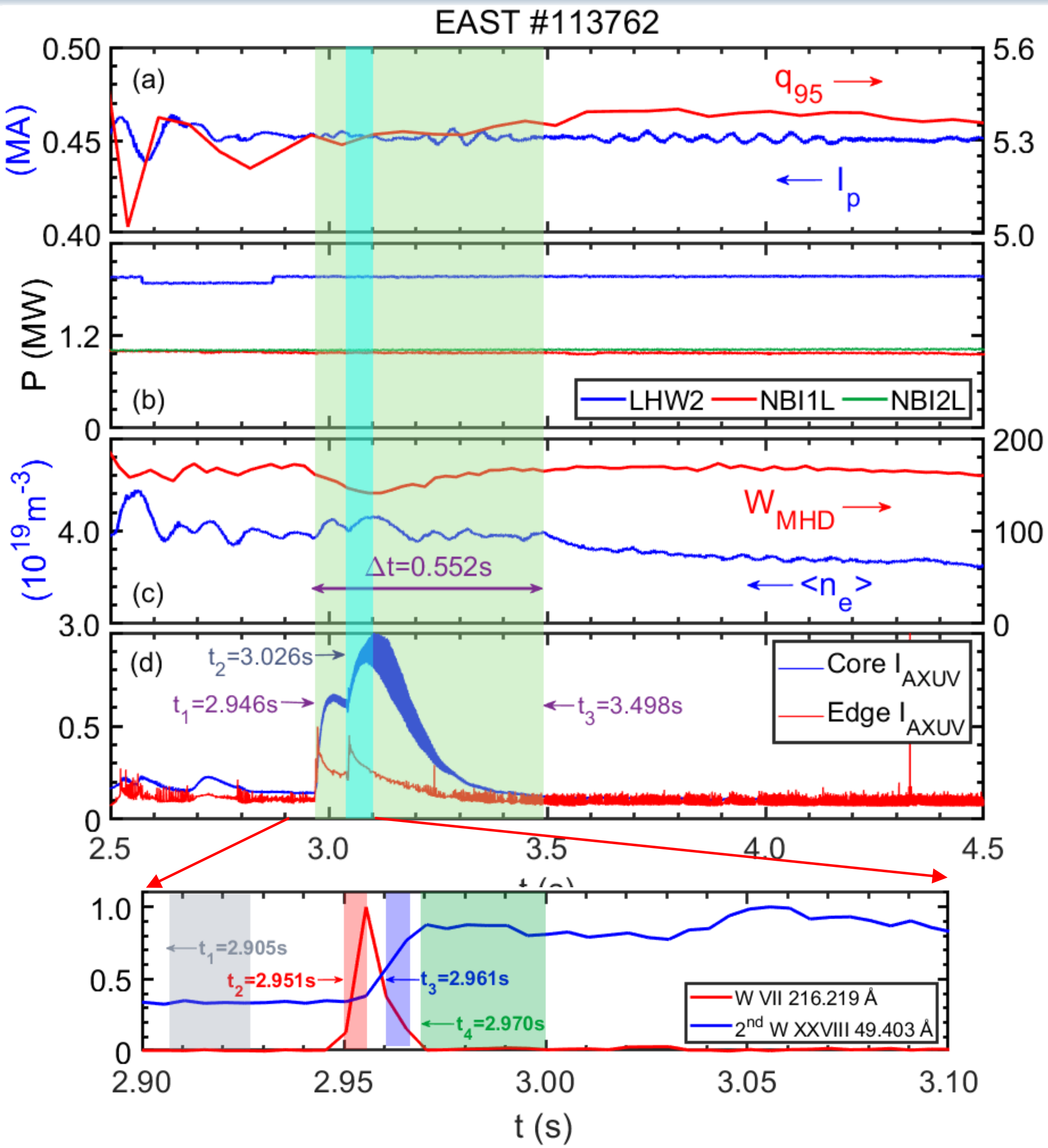

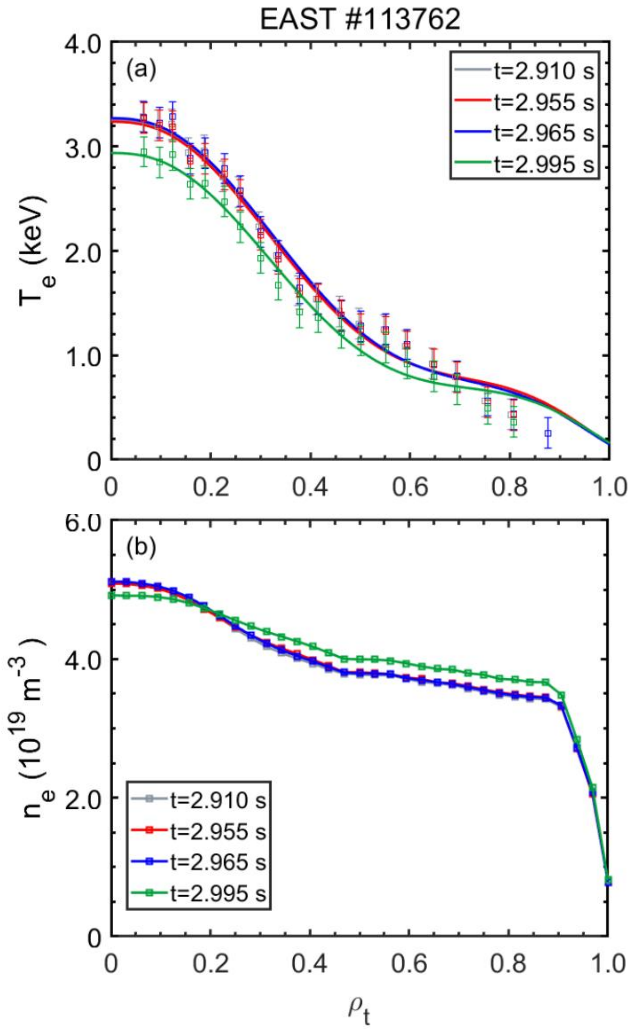

- Impurity sputtering events occurred at t=2.946 s.

Glance at the full W spectra in 5-130 Å

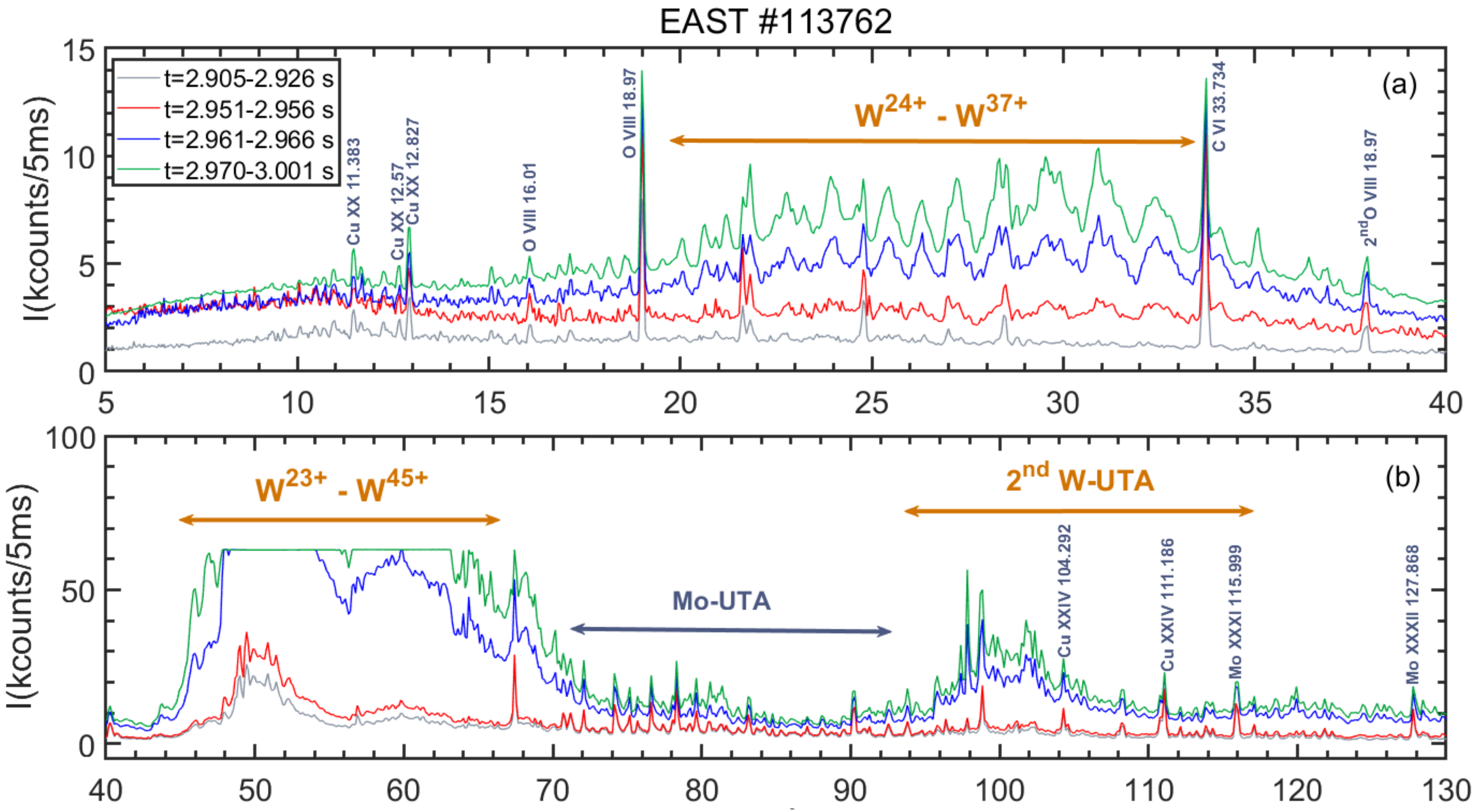

- The discharge with strong W radiation is helpful to identify the lines from weekly ionized W ions
- 2nd and 3rd W-UTA are helpful to identify the fine structure of W-UTA

Glance at the full W spectra in 130-480 Å

ASIPP

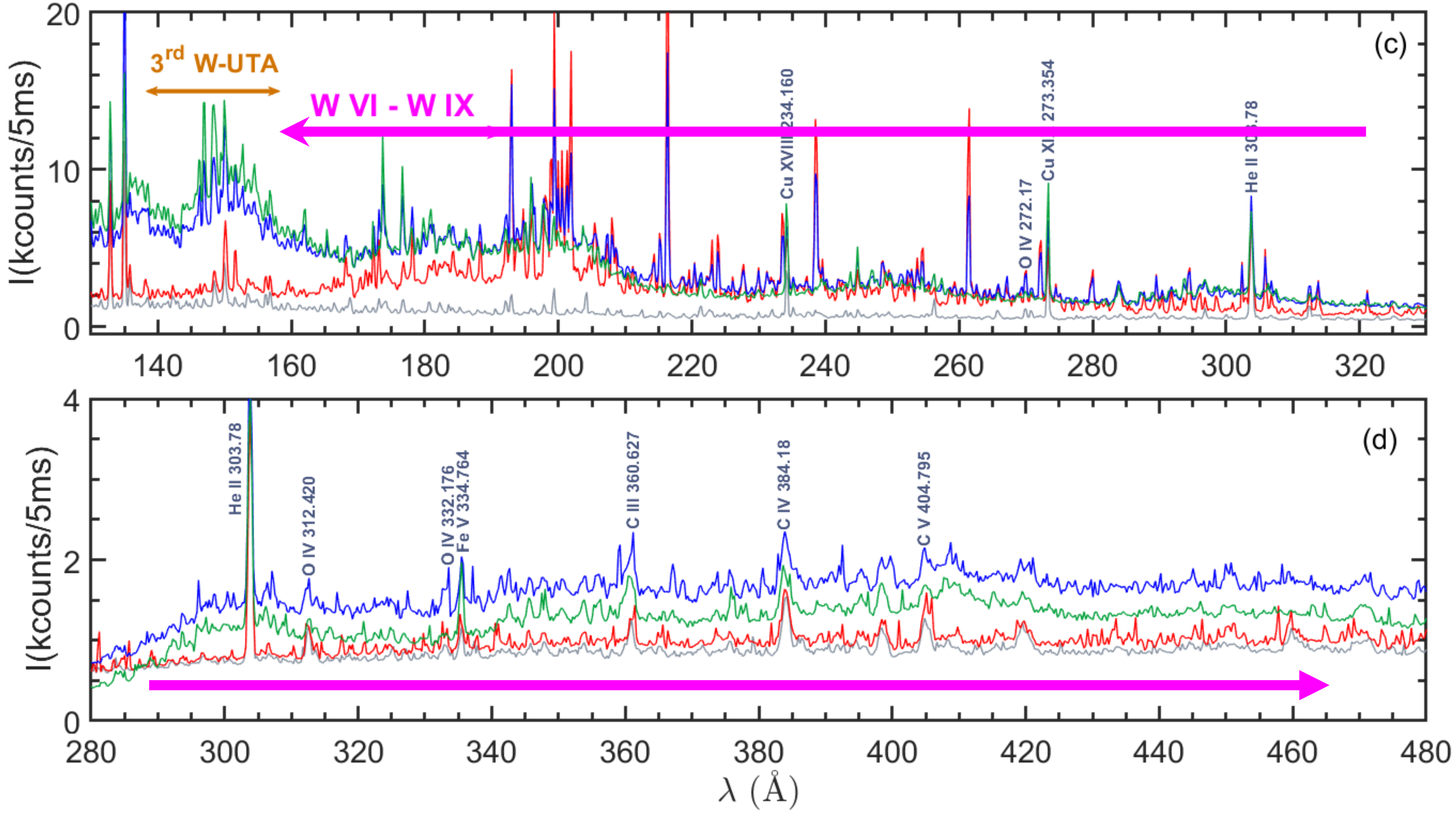

- A lot of W^{5+}-W^{8+} lines appear at longer λ

W lines identification at 130-220 Å

ASIPP

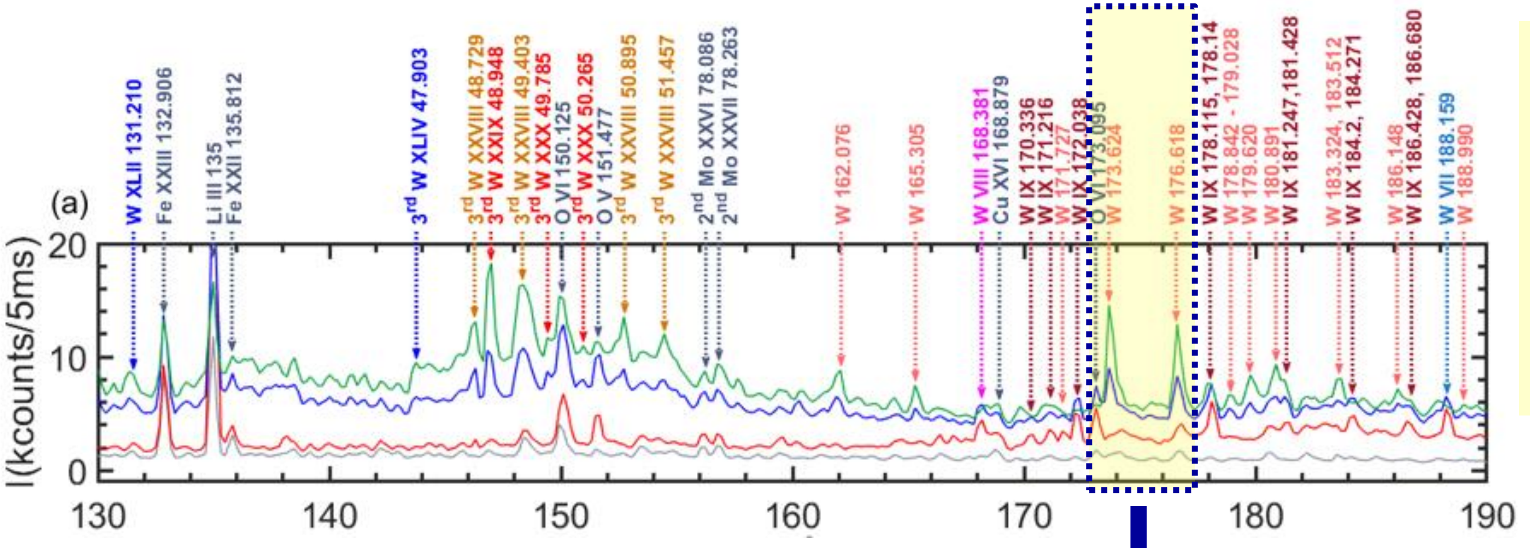

Isolated and strong new W lines

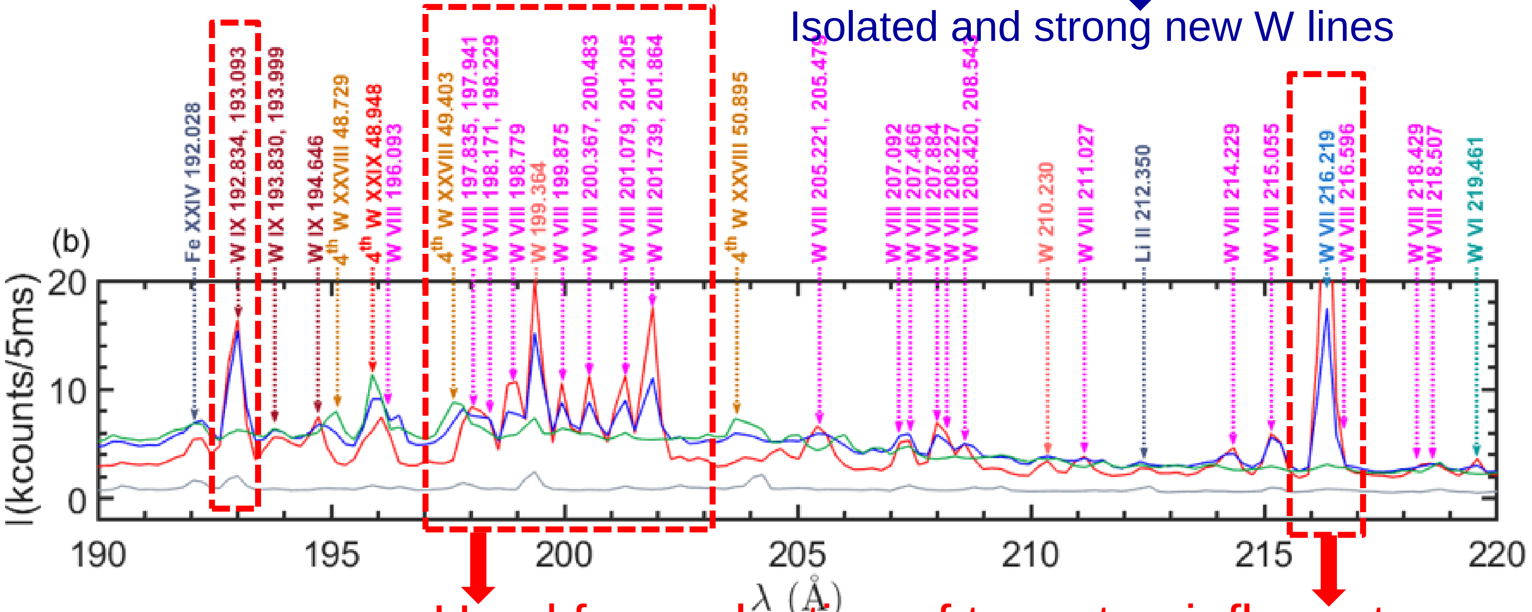

Used for evaluation of tungsten influx rate

- **W IX (W^{8+}), W VIII (W^{7+}), and W VII (W^{6+})**
- Several lines from **W^{8+}** and **W^{7+}** ions are identified referring to the results from a vacuum spark.
- **W^{6+} ions** are identified based on NIST, fusion devices.

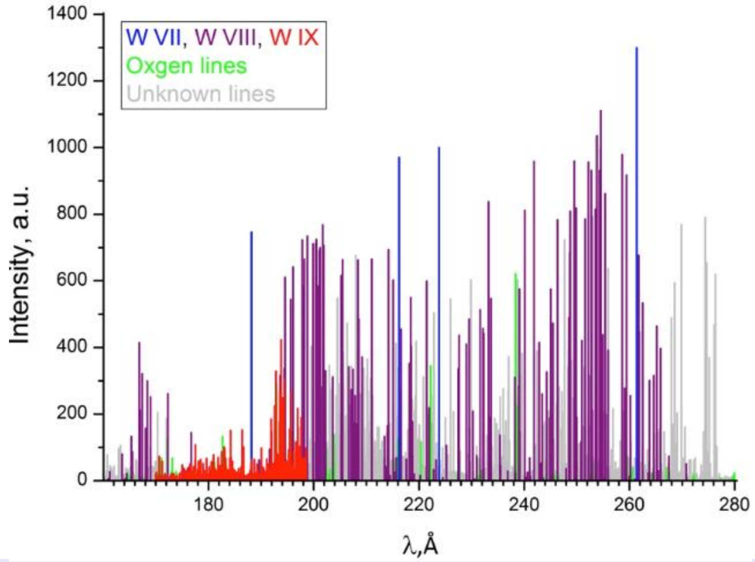

✓ Clementson J. 2010 *J. Phys. B: At. Mol. Opt. Phys.* 43 144009
✓ Clementson J. *et al* 2015 *Atoms* 3 407-421
✓ Ryabtsev A. *et al* 2015 *Atoms* 3 273-298

W lines identification at 220-330 Å

ASIPP

Used for evaluation of tungsten influx rate

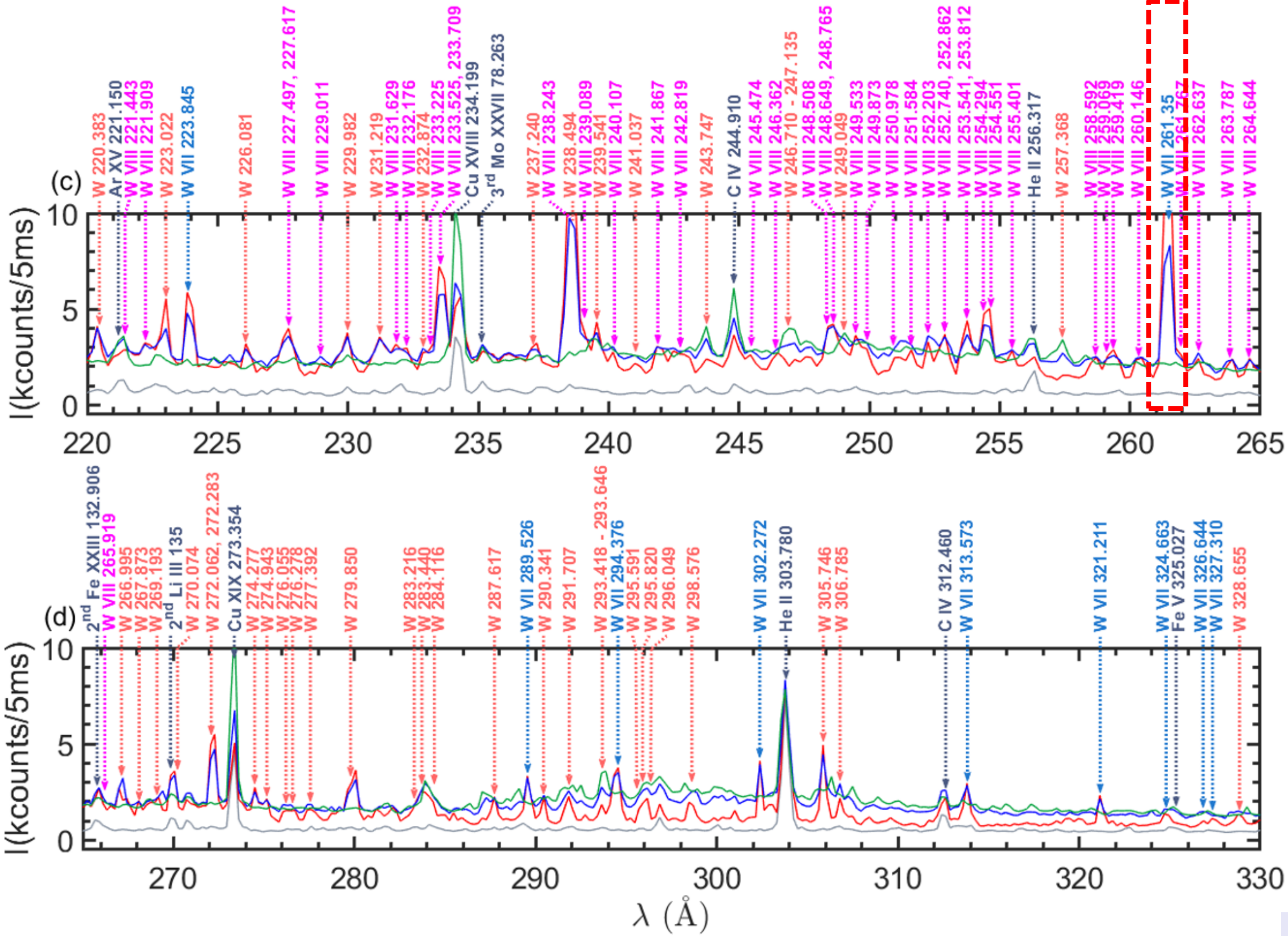

- Newly discovered W lines are indicated by light red labels.
- **Several W^{6+} lines at 289-330 Å** are identified referring to NIST, SSPX.

SSPX

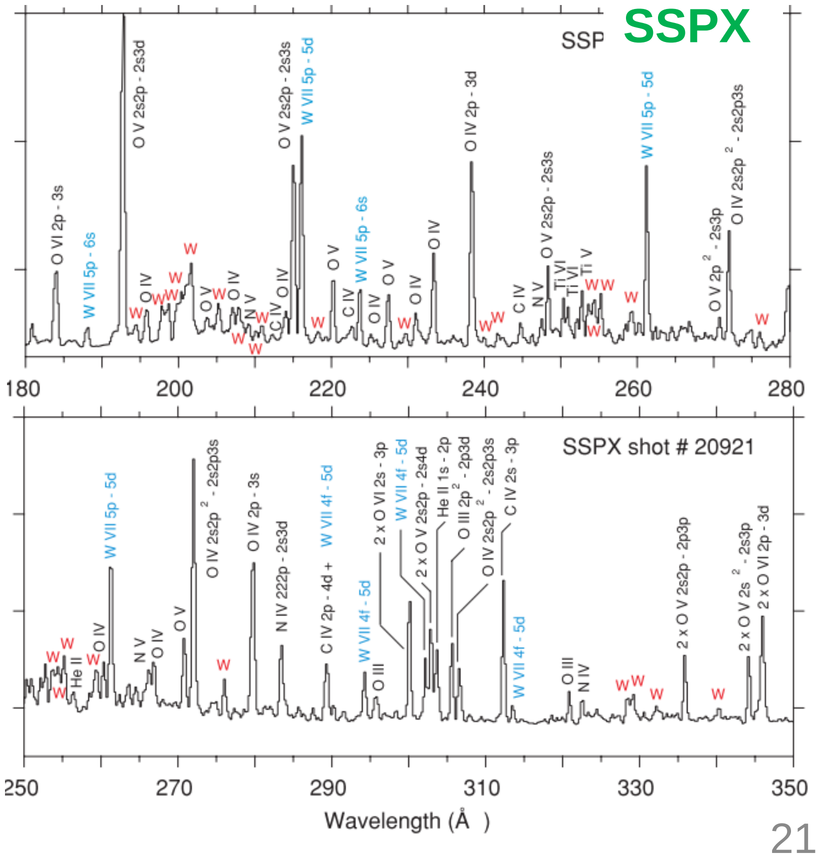

✓ Clementson J. 2010 *J. Phys. B: At. Mol. Opt. Phys.* 43 144009

Observation and identification of W ions with low ionization stages in a discharge with tungsten sputtering (T_{e0}=1.1keV)

ASIPP

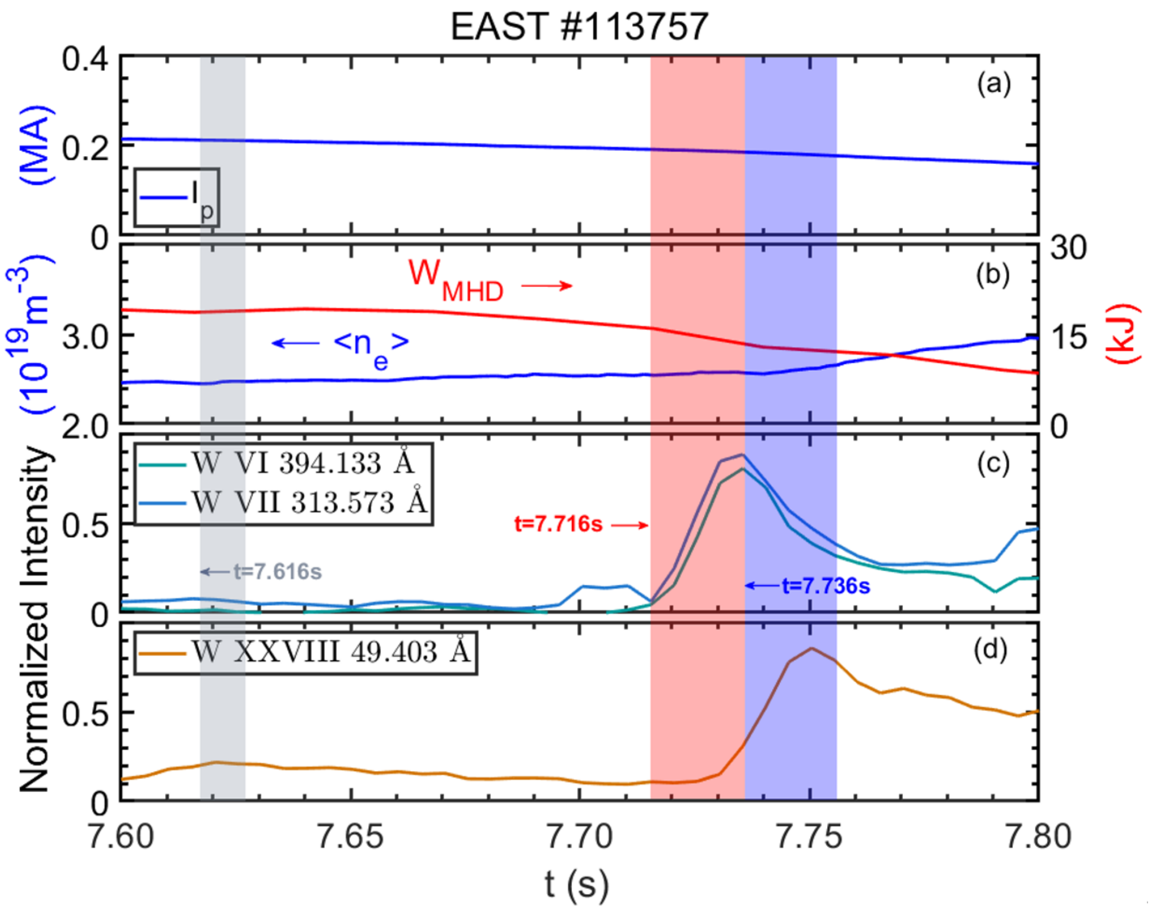

Radial profiles of T_e

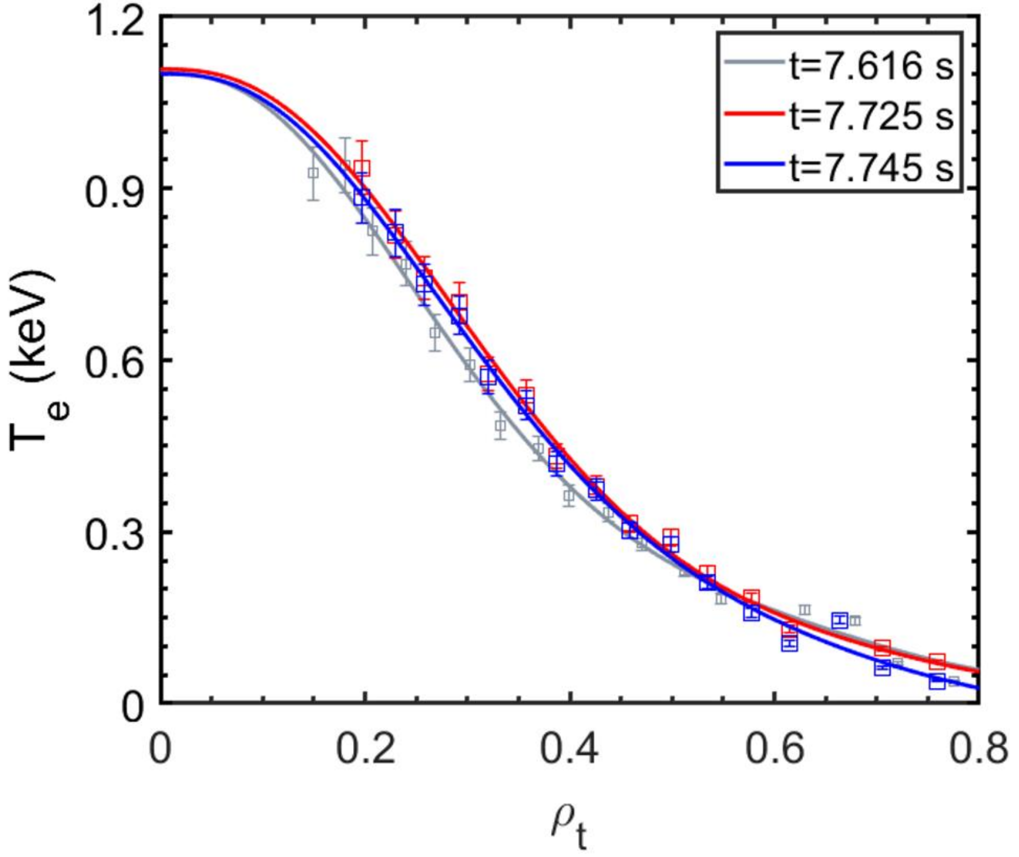

- W sputtering events occurred at t=7.716 s.

- T_e is basically sustained

Glance at the EUV spectra in 5-130 Å

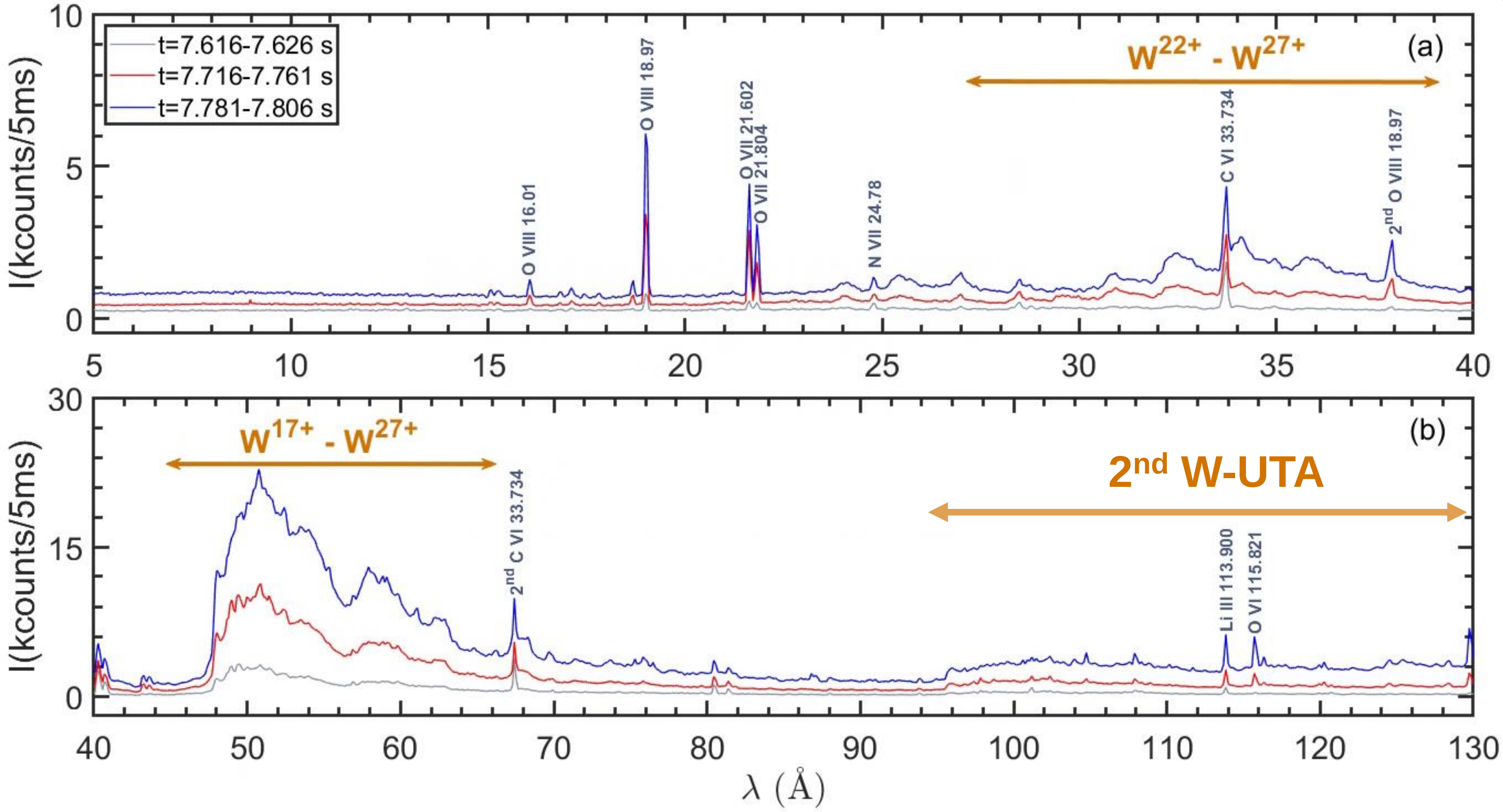

- W-UTA are composed of W^{22+}- W^{27+} in 25-40 Å band and W^{17+}- W^{27+} in 45-75 Å band at T_{e0}=1.1 keV, respectively.

Glance at the EUV spectra in 130-480 Å

ASIPP

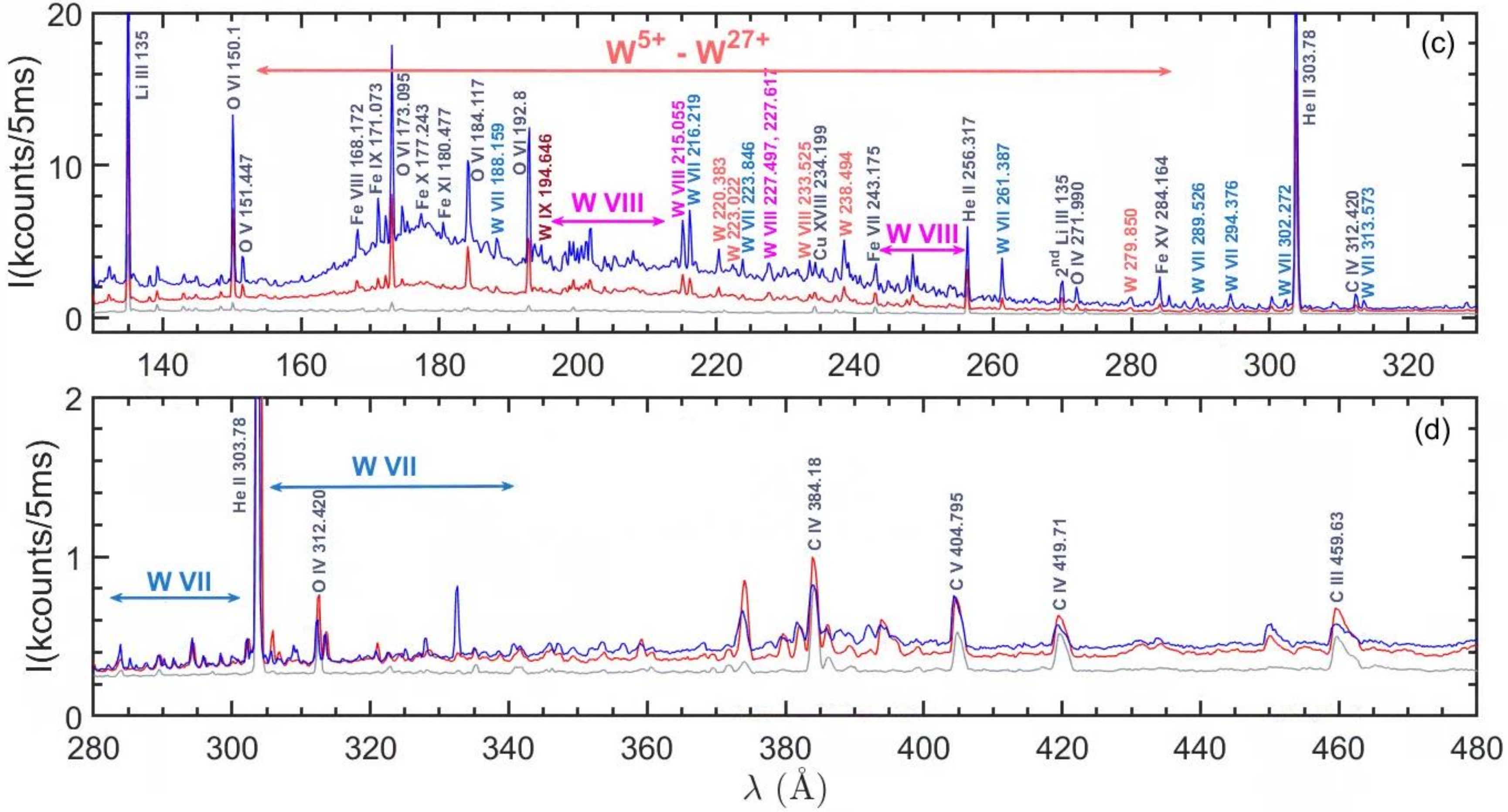

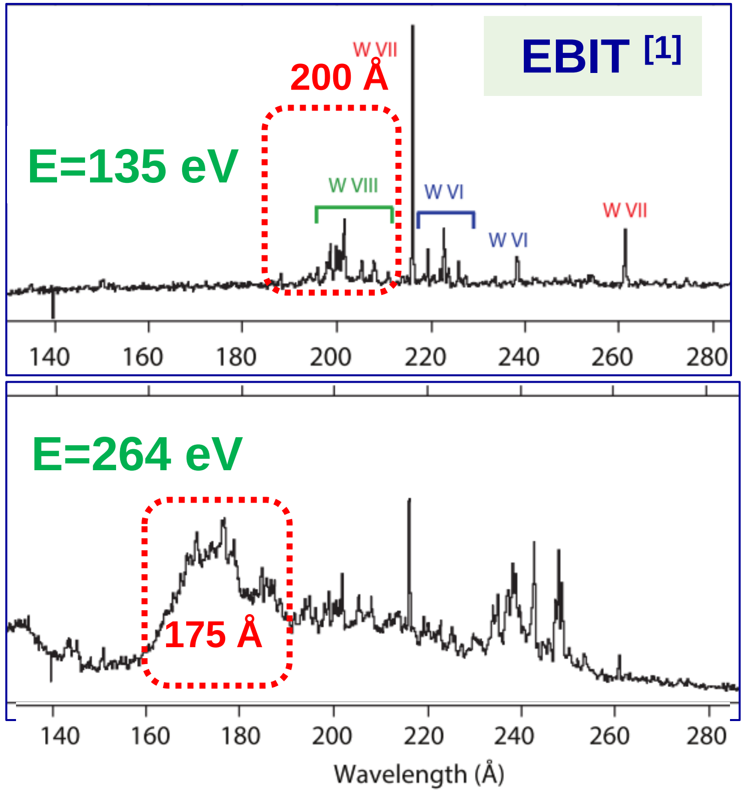

[1] Clementson J. 2015 *Atoms* 3 407-421

- W-UTA at 150-280 Å could be composed of W^{5+}-W^{27+} referring to previous results in LHD[2].
- The peak position of W-UTA moves from ~200 Å to ~175 Å region at T_{e0}=1.0 keV.
- When T_{e0} is 1.0 keV, a lot of W lines measured by EUV_Long_b appear in the wavelength range of 280-480 Å.

[2] Harte C.S. *et al* 2011 *J. Phys. B: At. Mol. Opt. Phys.* 44 175004

W line identification in 280-480 Å at low T_e

ASIPP

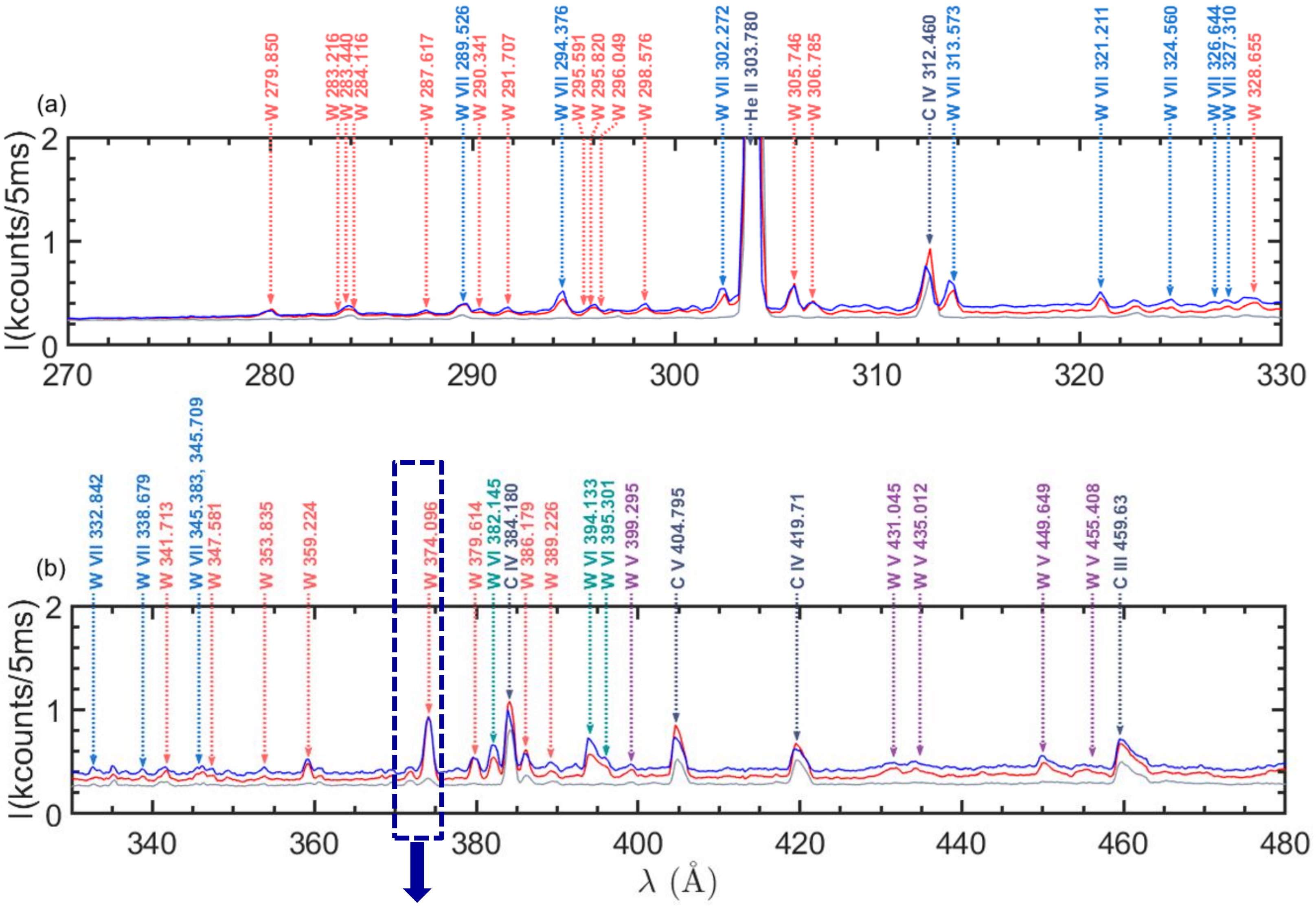

Isolated and strong new W lines

- W VII (W^{6+}), W VI (W^{5+}), W V (W^{4+})
- W^{5+} and W^{4+} ions are identified based on NIST database.
- W VI at 382.145 Å, 394.133 Å, and 395.301 Å are observed.

✓ Clementson J. *et al* 2010 *J. Phys. B: At. Mol. Opt. Phys.* 43 144009
✓ Clementson J. *et al* 2015 *Atoms* 3 407-421
✓ Kramida A.E. *et al* 2009 *Atomic Data and Nuclear Data Tables* 95 305-474

Evolution of W-UTA at 150-280 Å

ASIPP

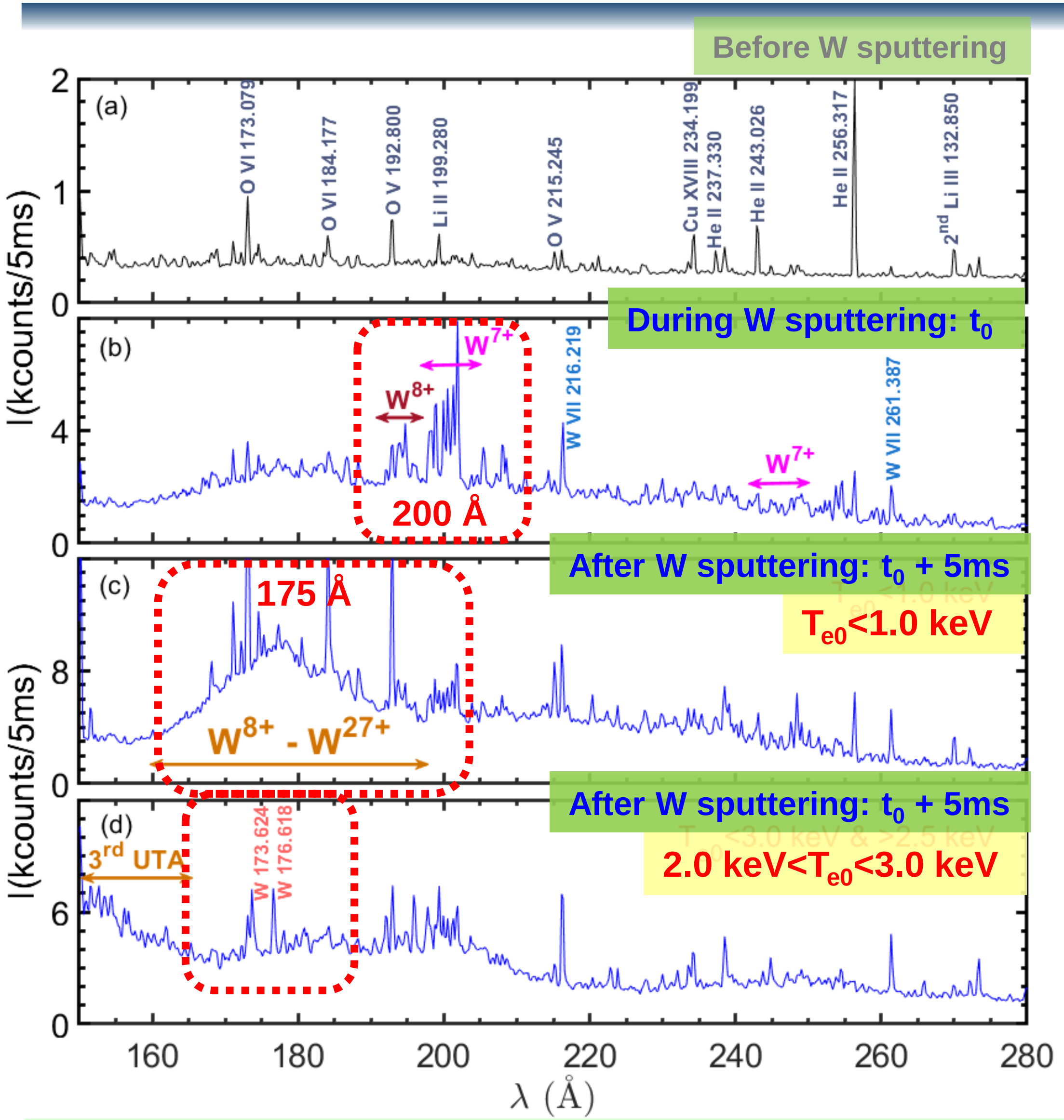

- During W sputtering, the peak position of W-UTA remains in the 200 Å region, regardless of T_{e0}.
- When T_{e0} <1.0 keV, after t_0+5ms, the peak location of W-UTA moves from 200 Å to 175 Å region.
- When 2.0<T_{e0} <3.0 keV, the peak intensity in the 200 Å region decrease after t_0+5ms, while two isolated W lines from higher ionization ions (173.624 Å and 176.618 Å) appear in the 175 Å region.

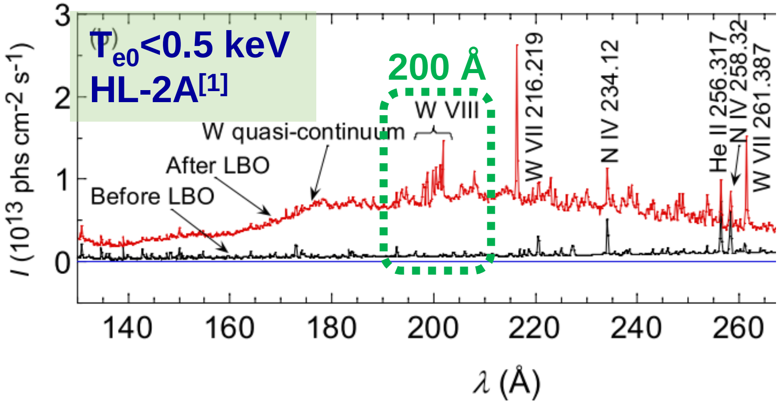

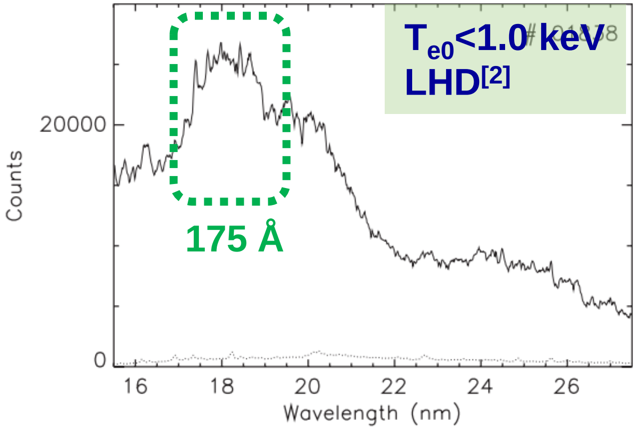

□ Probably the feature of spectra depend on edge plasma confinement

[1] Dong C.F. *et al* 2019 *Nucl. Fusion* 59 016020

[2] Harte C.S. 2011 *J. Phys. B: At. Mol. Opt. Phys.* 44 175004

Several W^{4+}-W^{7+} lines appearing with strong intensity chosen for tungsten influx evaluation

ASIPP

Wq+	λ (Å)		Transitions		
	This work	Database	Relative (counts/5ms)	Lower level	Upper level
W VIII (W^{7+})	201.700 ± 0.02	201.739[a]	11720[A]	$4f^{13}5p^6\ ^2F_{7/2}$	$4f^{13}5p^5 5d$ 9/2
W VII (W^{6+})	216.351 ± 0.01	216.219[b]	34550[A]	$4f^{14}5p^6\ ^1S_0$	$4f^{14}5p^5(^2P^\circ_{1/2})5d\ (1/2,3/2)^\circ_1$
	223.836 ± 0.01	223.846[b]	5872[A]	$4f^{14}5p^6\ ^1S_0$	$4f^{14}5p^5(^2P^\circ_{3/2})6s\ (3/2,1/2)^\circ_1$
	261.317 ± 0.01	261.387[b]	13900[A]	$4f^{14}5p^6\ ^1S_0$	$4f^{14}5p^5(^2P^\circ_{3/2})5d\ (3/2,5/2)^\circ_1$
W VI (W^{5+})	382.133 ± 0.04	382.145[b]	661[B]	$5d\ ^2D_{3/2}$	$5f\ ^2F^\circ_{5/2}$
	394.072 ± 0.04	394.133[b]	713[B]	$5d\ ^2D_{5/2}$	$5f\ ^2F^\circ_{7/2}$
W V (W^{4+})	449.673 ± 0.05	449.649[b]	549[B]	$5d^2\ ^3P_1$	$5d(^2D_{5/2})5f\ (5/2,5/2)^\circ_2$

- Influx of W^{Z+} should be more accurate than W^0 source when we considering the source of core tungsten
- Influx of W^{6+} has been estimated in HL-2A for W injected by LBO

Outline

- Background & Motivation
- Tungsten spectroscopic diagnostics
- Tungsten line identification and density profiles
- Tungsten influx evaluation: S/XB calculation
- Summary & Future work

Introduction of S/XB

ASIPP

S/XB: Ionization Events per Photon

- The ratio of flux of ions (due to ionization) to the emission in a spectrum line integrated along a line of sight.

The flux of impurity which ionizes in the line–of–sight from a metastable level σ is

$$\Gamma = n_e\, S_\sigma \int n_\sigma(\xi)\, d\xi$$

The emissivity in a transition $j \to k$ is

$$\epsilon_{jk} = A_{jk}\, n_e\, n_j = A_{jk}\, n_e\, n_\sigma\, \mathcal{F}_{j\sigma}\,,$$

where $\mathcal{F}_{j\sigma}$ is the effective contribution to the population of the upper level j from excitation from the metastable σ.

$$\Gamma = n_e\, S_\sigma \int \frac{\epsilon_{jk}(\xi)}{A_{jk}\, n_e\, \mathcal{F}_{j\sigma}}\, d\xi = \frac{S_\sigma}{A_{jk}\, \mathcal{F}_{j\sigma}} \times \int \epsilon_{jk}(\xi)\, d\xi$$

$$\begin{aligned} \Gamma &= \frac{S_\sigma}{A_{jk}\, \mathcal{F}_{j\sigma}} \times \int \epsilon_{jk}(\xi)\, d\xi \equiv \mathcal{SXB}_{jk} \times \int \epsilon_{jk}(\xi)\, d\xi \\ &= \mathcal{SXB}_{jk} \times I_{jk} \end{aligned}$$

$$\mathcal{SXB}_{jk} = \frac{\Gamma}{I_{jk}} = \frac{S_\sigma}{A_{jk}\, \mathcal{F}_{j\sigma}}$$

- Electron-impact ionization
- Electron-impact excitation
- Radiative transition rates

For only one metastable, we need to calculate

$$\mathcal{SXB}_{\sigma,ji} = \frac{S_\sigma}{A_{ji}\mathcal{F}_{j\sigma}} \qquad N_j \equiv n_e N_\sigma \mathcal{F}_{j\sigma} \longrightarrow \mathcal{F}_{j\sigma} = \frac{1}{n_e}\frac{N_j}{N_\sigma}$$

For many metastables, we need to modify the expression to:

$$\mathcal{SXB}_{ji} = \frac{1}{A_{ji}}\left(\frac{S_\sigma}{\mathcal{F}_{j\sigma}} + \frac{S_\mu}{\mathcal{F}_{j\mu}} + \cdots\right)$$

and in this case, $\mathcal{F}_{j\sigma}$ is defined as

$$N_j \equiv n_e\left(N_\sigma \mathcal{F}_{j\sigma} + N_\mu \mathcal{F}_{j\mu} + \cdots\right)$$

S_σ: the ionization rate coefficient from metastable level σ

$F_{j\sigma}$: the effective contribution to the population of the upper level j from excitation of the metastable σ

A_{jk}: the radiative rate coefficient for the transition j to k

[1] K. Behringer PPCF 31, 2059 (1989)
[2] C. P. Ballance J. Phys B 46, 055202 (2013).

Simplest case: 3-levels model

C. P. Ballance J. Phys B 46, 055202 (2013).

$$\mathcal{F}_{31} = \frac{Q_{13}(A_{21}+n_eQ_{21}+n_eQ_{23})+n_e\,Q_{12}\,Q_{23}}{n_eQ_{23}(A_{32}+n_eQ_{32})+(A_{21}+n_eQ_{21}+n_eQ_{23})(A_{31}+A_{32}+n_eQ_{31}+n_eQ_{32})}$$

For $n_e < 10^{14}$ cm^{-3}, $(n_eQ_{31} + n_eQ_{32}) << A_{31}+A_{32}$

$$\begin{aligned}
\mathcal{F}_{31} &\approx \frac{Q_{13}(A_{21}+n_eQ_{21}+n_eQ_{23})+n_e\,Q_{12}\,Q_{23}}{(A_{21}+n_eQ_{21}+n_eQ_{23})(A_{31}+A_{32})} \\
&= \frac{Q_{13}(A_{21}+n_eQ_{21}+n_eQ_{23})}{(A_{21}+n_eQ_{21}+n_eQ_{23})(A_{31}+A_{32})} + \frac{n_e\,Q_{12}\,Q_{23}}{(A_{21}+n_eQ_{21}+n_eQ_{23})(A_{31}+A_{32})} \\
&\approx \frac{Q_{13}}{(A_{31}+A_{32})} + \frac{n_e\,Q_{12}\,Q_{23}}{(A_{21}+n_eQ_{21})(A_{31}+A_{32})}
\end{aligned}$$

Low density limit ($n_e < 10^6$ cm^{-3}, depending on the line) $\quad \mathcal{F}_{31} = \dfrac{Q_{13}}{(A_{31}+A_{32})}$

Intermediate density plateau, $A_{21} << n_eQ_{21}$ $\quad \mathcal{F}_{31} \sim \dfrac{Q_{13}}{(A_{31}+A_{32})} + \dfrac{Q_{12}\,Q_{23}}{Q_{21}\,(A_{31}+A_{32})}$

Test: S/XB calculation for 3 VUV lines (1)

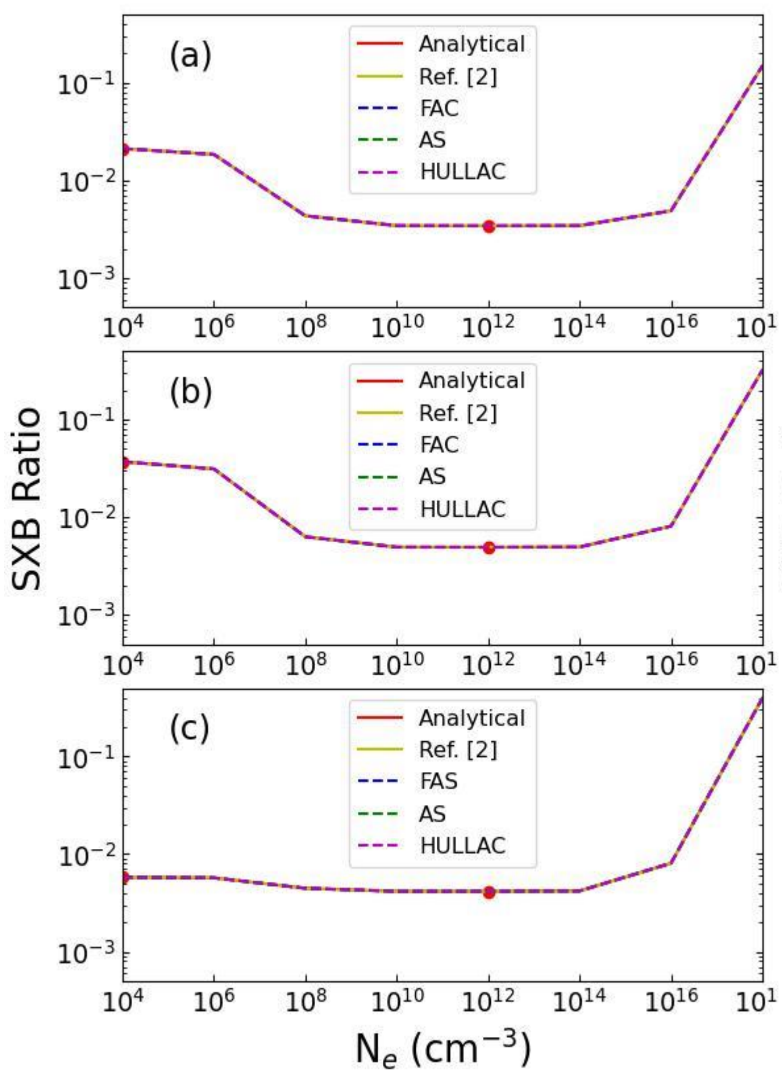

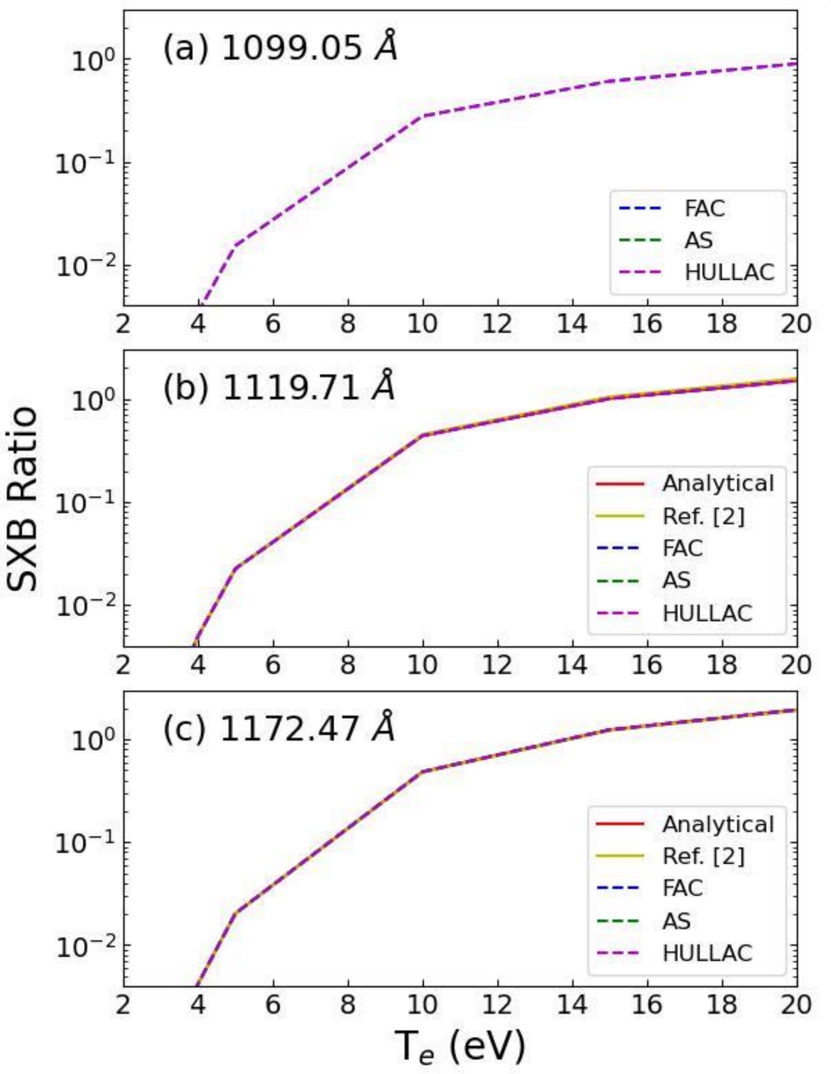

- S, A and Q from Ref. [2].
- CRM include 3 levels, and only one metastable level included in $F_{j,\sigma}$.

[2] C. P. Ballance J. Phys B 46, 055202 (2013).

- ➢ SXB (n_e) at T_e = 4 eV
- ➢ Lines: 1099.05, 1119.71 and1172.47 Å.

- ➢ SXB (T_e) at $n_e = 1\times10^{14}$ cm^{-3}
- ➢ Lines: 1099.05, 1119.71 and1172.47 Å.

Test: S/XB calculation for 3 VUV lines (2)

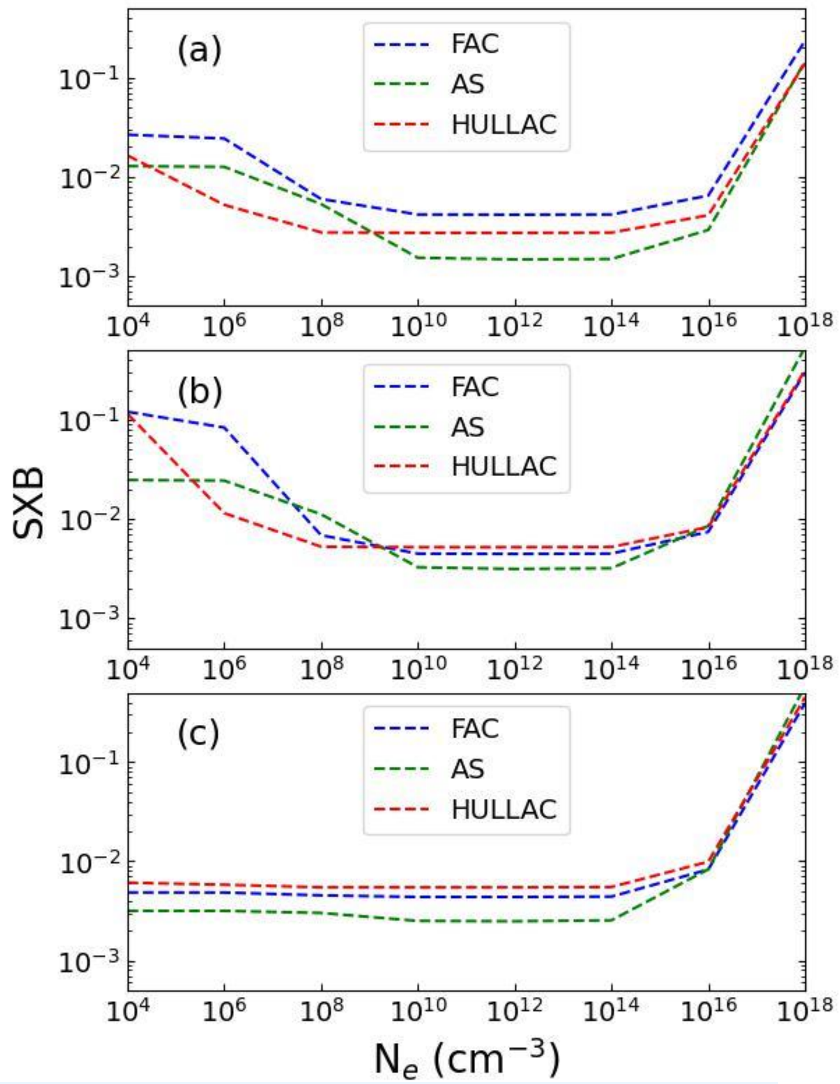

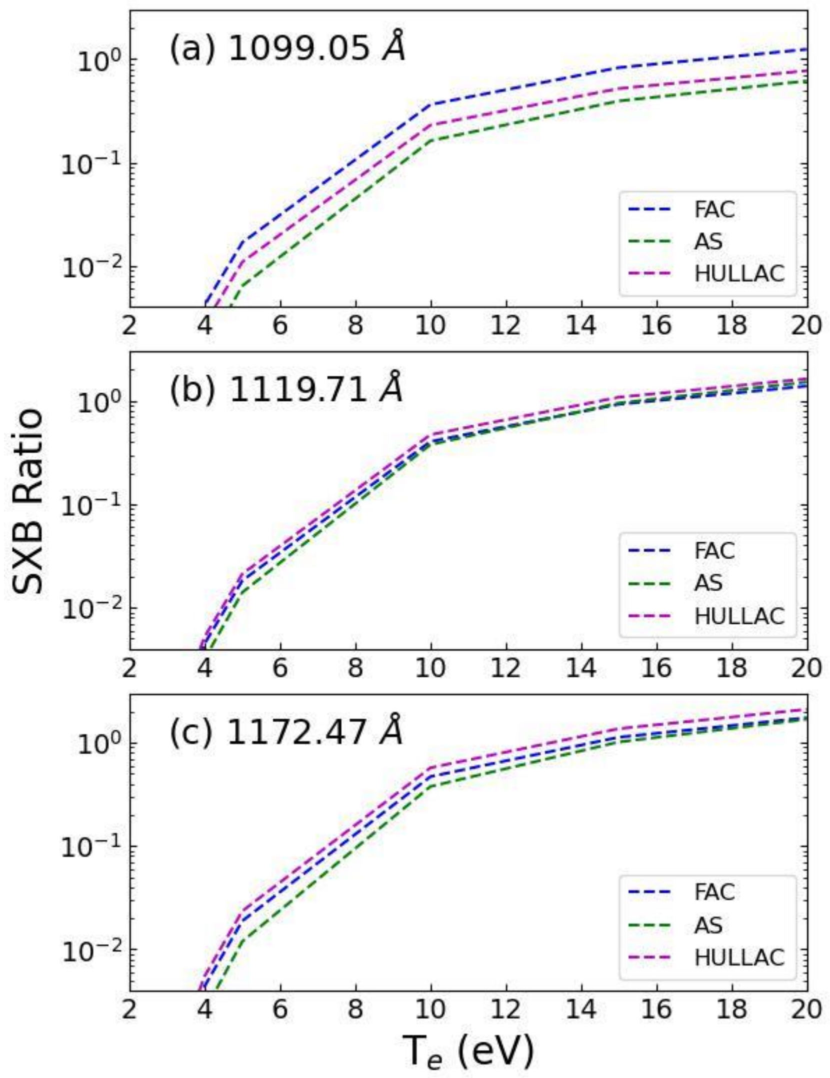

- S from Ref. [2]
- A and Q from FAC, AutoStructure and HULLAC.
- CRM include 3 levels, and only one metastable level included in $F_{j,\sigma}$.

- SXB (n_e) at T_e = 4 eV
- Lines: 1099.05, 1119.71 and1172.47 Å.

- SXB (T_e) at $n_e = 1 \times 10^{14}$ cm^{-3}
- Lines: 1099.05, 1119.71 and1172.47 Å.

Test: S/XB calculation for 3 VUV lines (3)

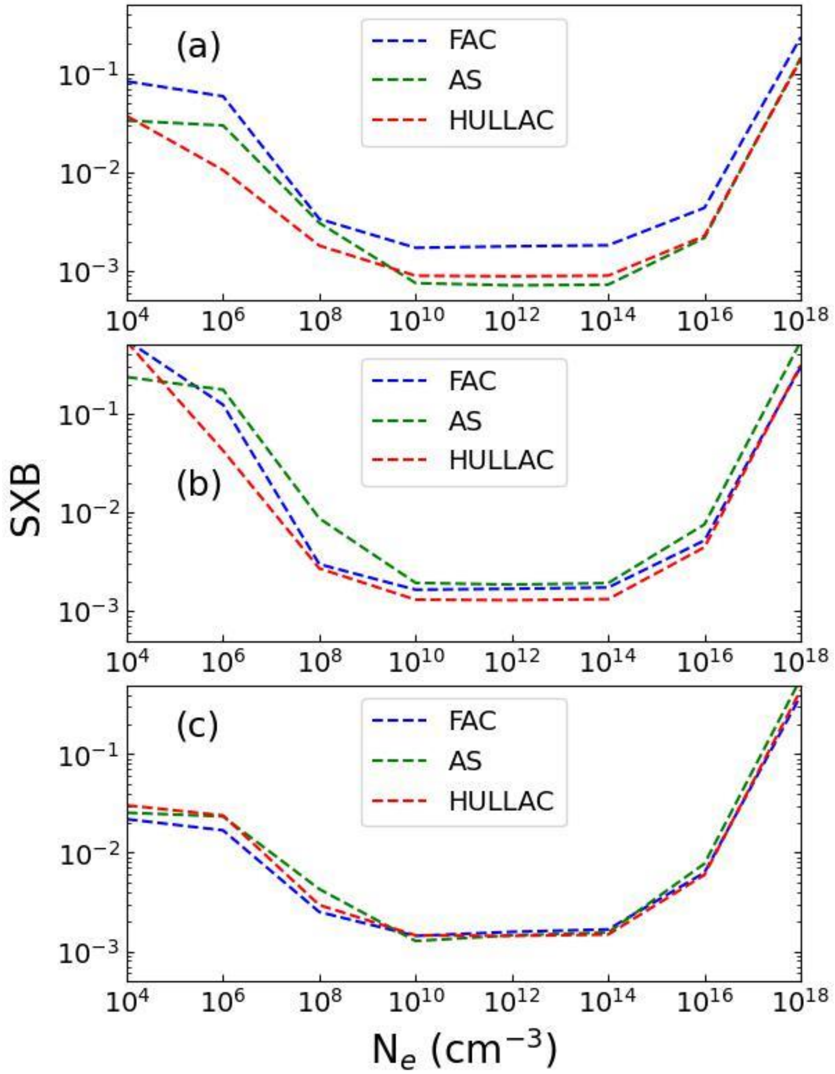

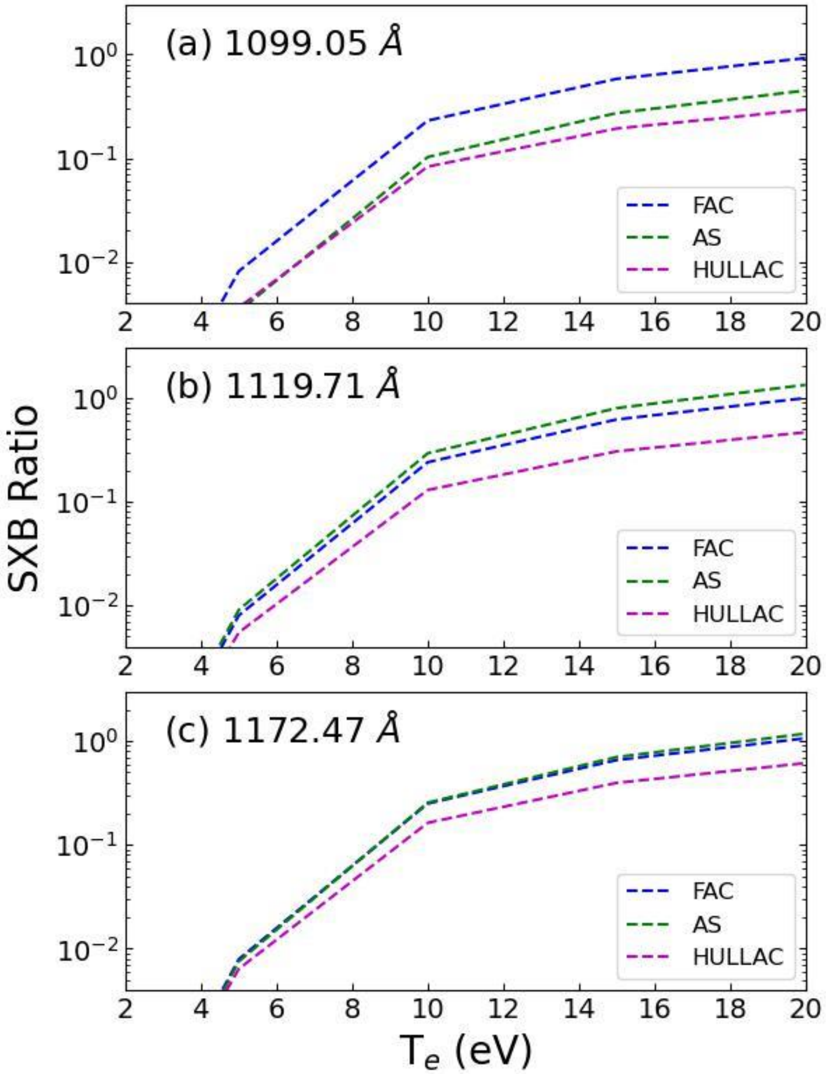

- S from Ref. [2]
- A and Q are from FAC, AutoStructure and HULLAC.
- **CRM include 82 levels**, and only one metastable level included in $F_{j,\sigma}$.

- SXB (n_e) at T_e = 4 eV
- Lines: 1099.05, 1119.71 and1172.47 Å.

- SXB (T_e) at n_e = 1×10^{14} cm^{-3}
- Lines: 1099.05, 1119.71 and1172.47 Å.

Preliminary W influx evaluation in EAST

ASIPP

Wq+	λ (Å)		Transitions		
	This work	Database	Relative (counts/5ms)	Lower level	Upper level
W VIII (W^{7+})	201.700 ± 0.02	201.739[a]	11720[A]	$4f^{13}5p^6\ ^2F_{7/2}$	$4f^{13}5p^5 5d$ 9/2
W VII (W^{6+})	216.351 ± 0.01	216.219[b]	34550[A]	$4f^{14}5p^6\ ^1S_0$	$4f^{14}5p^5(^2P^\circ_{1/2})5d\ (1/2,3/2)^\circ_1$
	223.836 ± 0.01	223.846[b]	5872[A]	$4f^{14}5p^6\ ^1S_0$	$4f^{14}5p^5(^2P^\circ_{3/2})6s\ (3/2,1/2)^\circ_1$
	261.317 ± 0.01	261.387[b]	13900[A]	$4f^{14}5p^6\ ^1S_0$	$4f^{14}5p^5(^2P^\circ_{3/2})5d\ (3/2,5/2)^\circ_1$
W VI (W^{5+})	382.133 ± 0.04	382.145[b]	661[B]	$5d\ ^2D_{3/2}$	$5f\ ^2F^\circ_{5/2}$
	394.072 ± 0.04	394.133[b]	713[B]	$5d\ ^2D_{5/2}$	$5f\ ^2F^\circ_{7/2}$
W V (W^{4+})	449.673 ± 0.05	449.649[b]	549[B]	$5d^2\ ^3P_1$	$5d(^2D_{5/2})5f\ (5/2,5/2)^\circ_2$

The S/XB calculation for W^{4+}, W^{5+}, W^{6+} and W^{7+} ions:

- S from OPEN ADAS
- A and Q are from FAC and AutoStructure
- CRM include full levels
- But only one metastable level include in $F_{j,\sigma}$

- ✓ generates an ADF04 files, compatible with ADAS
- ✓ construct the population matrix
- ✓ solve the level population
- ✓ produce a synthetic spectra based on the emissivity of each line (n_j*A_{ji})

Preliminary W influx evaluation in EAST (W^{4+})

ASIPP

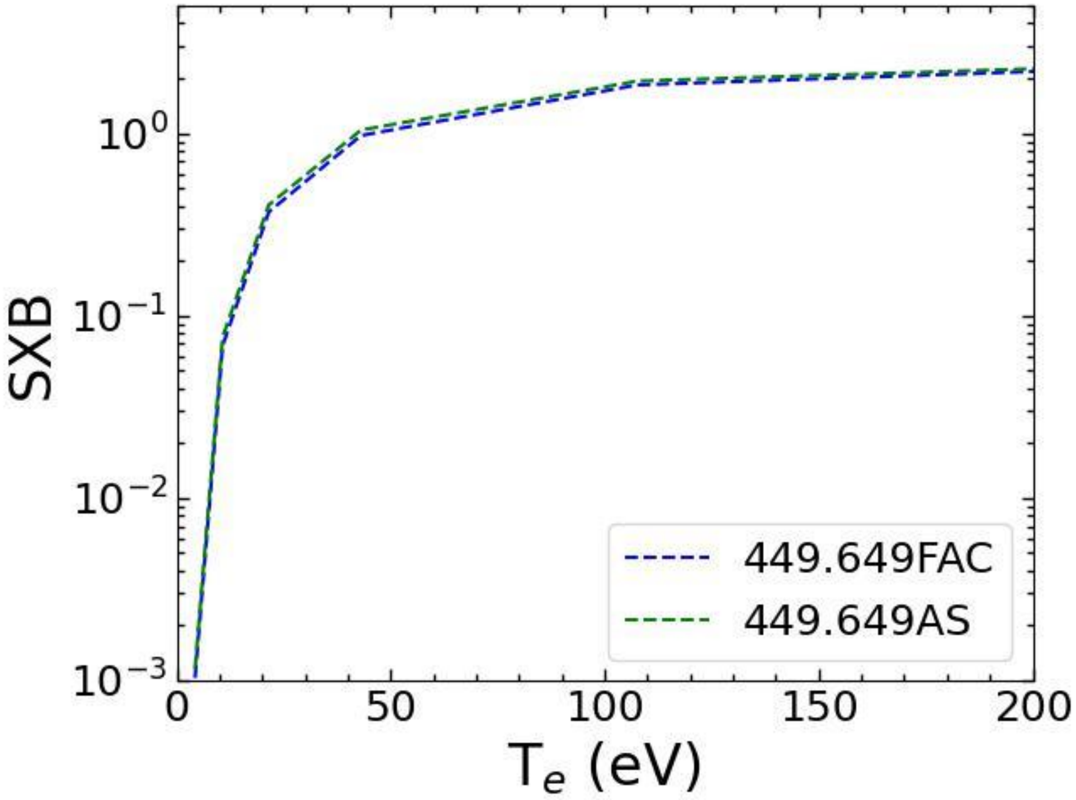

- SXB (T_e) at a $n_e = 1 \times 10^{14}$ cm^{-3},
- Line: W^{4+} at 449.649 Å.

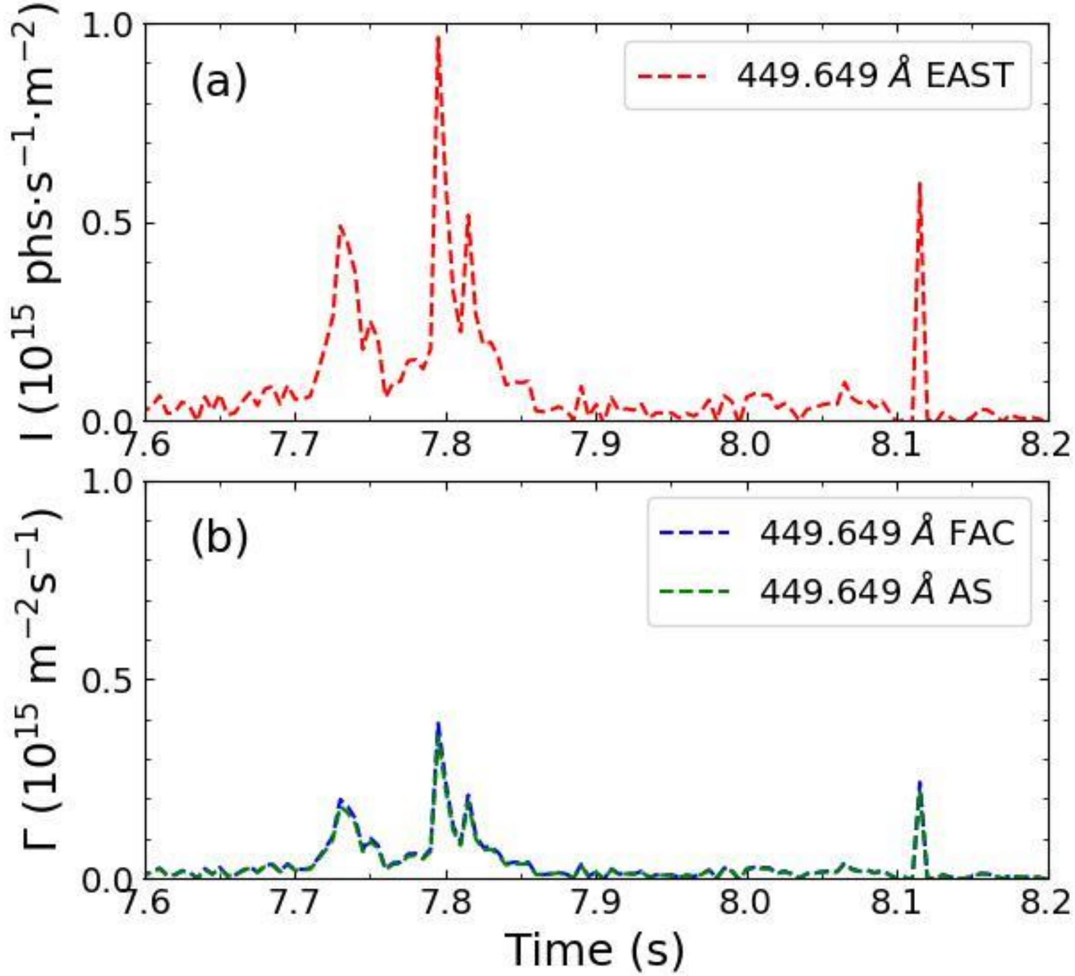

(a) Line intensity observed in EAST #113757

(b) W^{4+} influx evaluated from line 449.649 Å at T_e=10.8eV

Preliminary W influx evaluation in EAST (W^{5+})

ASIPP

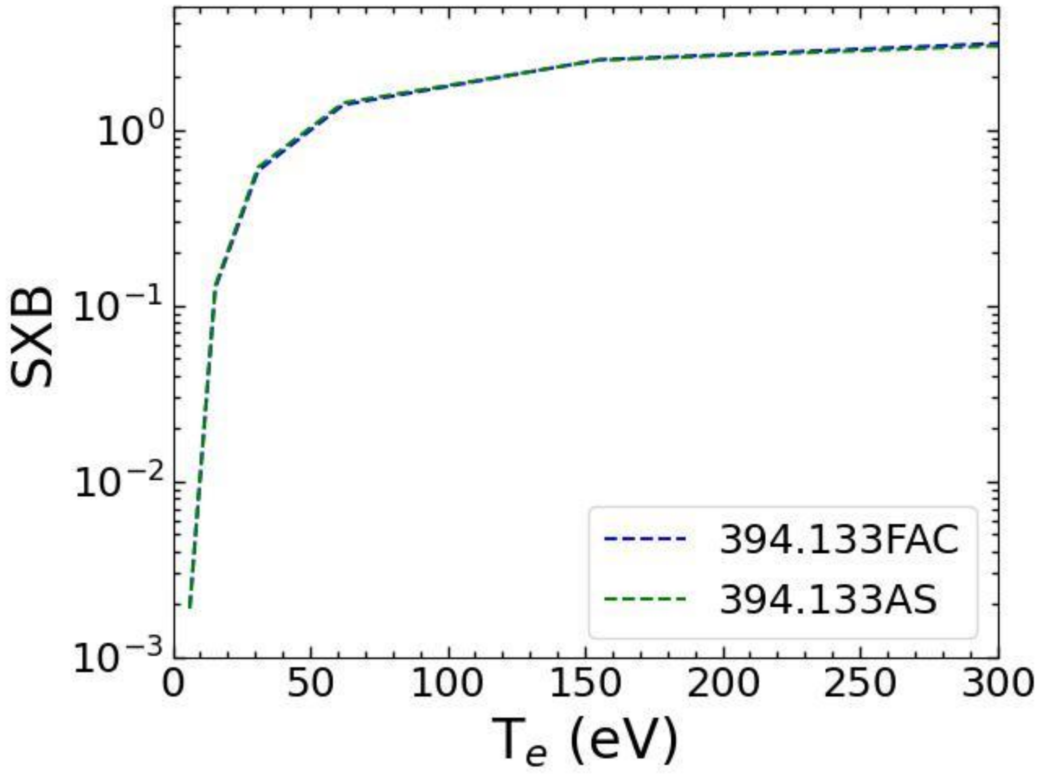

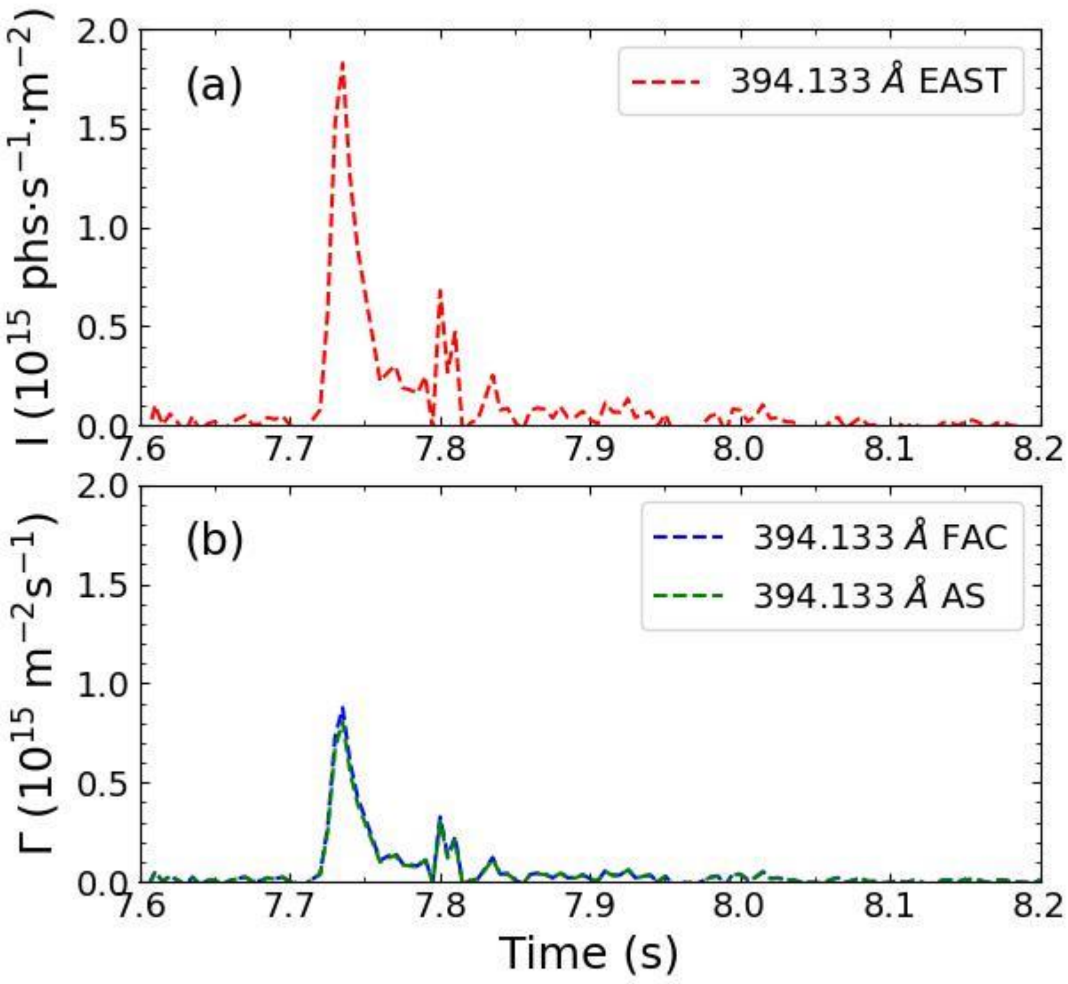

- SXB (T_e) at a $n_e = 1\times10^{14}$ cm^{-3}
- Line: W^{5+} at 394.133 Å

(a) Line intensity observed in EAST #113757

(b) W^{5+} influx evaluated from line 394.133 Å at T_e=15.5eV

Preliminary W influx evaluation in EAST (W^{6+})

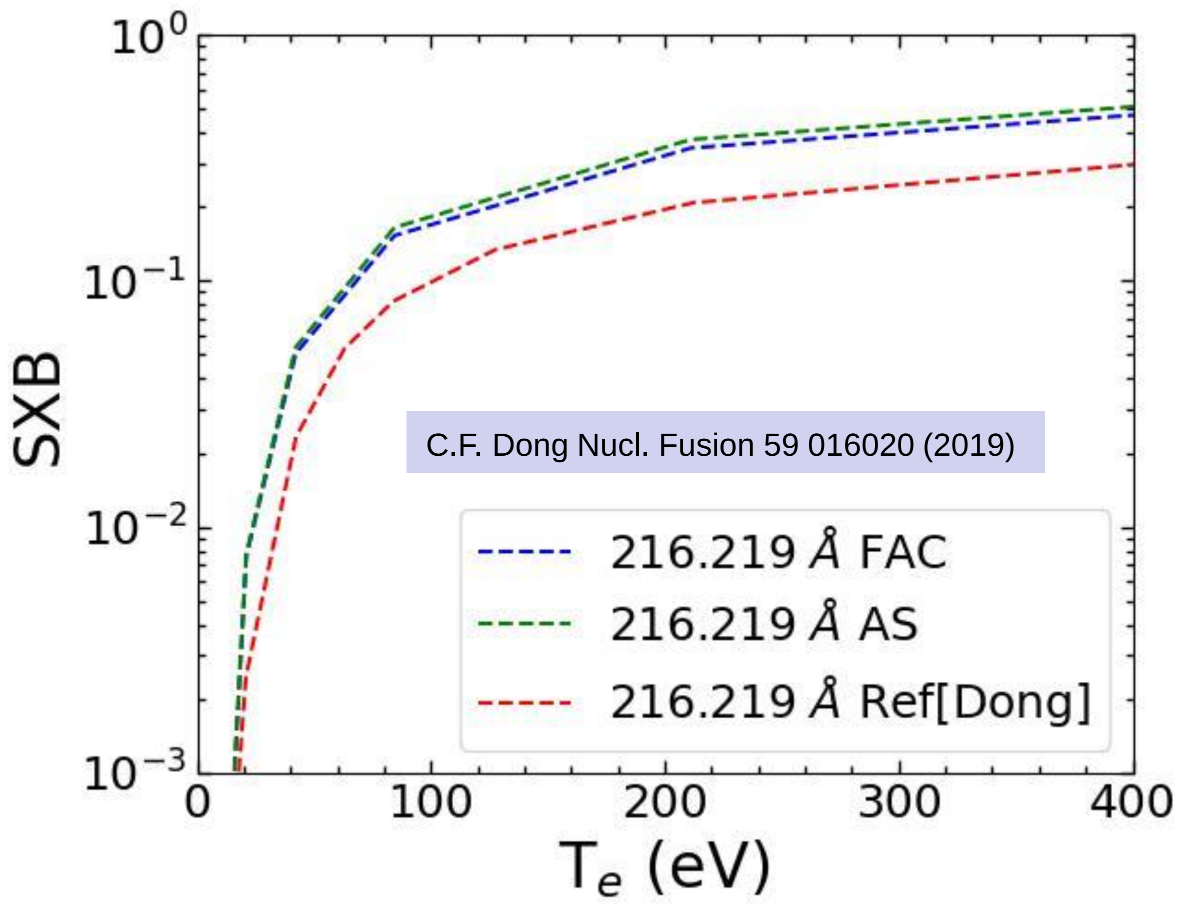

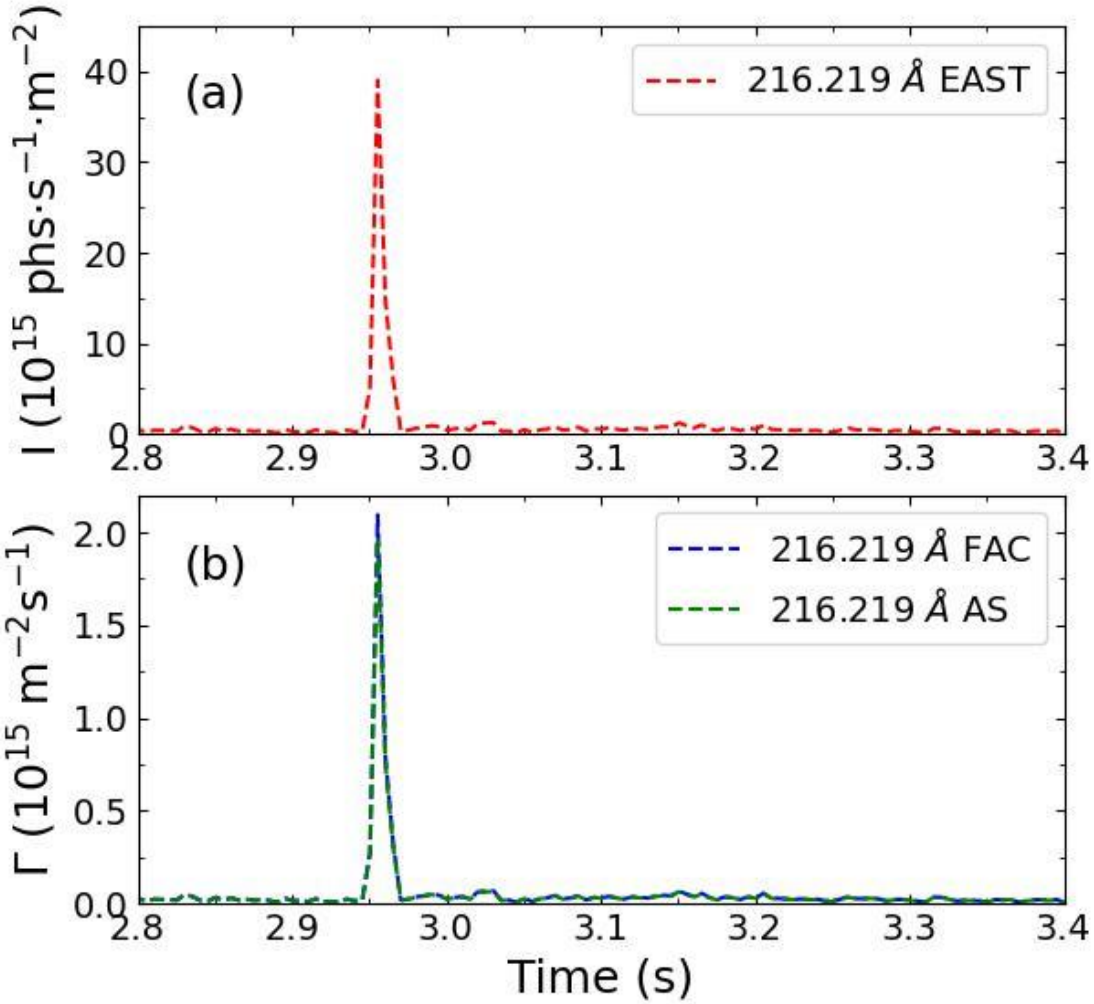

- SXB (T_e) at a n_e = 1×10^{13} cm^{-3}
- Line: W^{6+} at 216.219 Å

(a) Line intensity observed in EAST #113762

(b) W^{6+} influx evaluated from line 216.219 Å at T_e=21.1eV

Preliminary W influx evaluation in EAST (W^{7+})

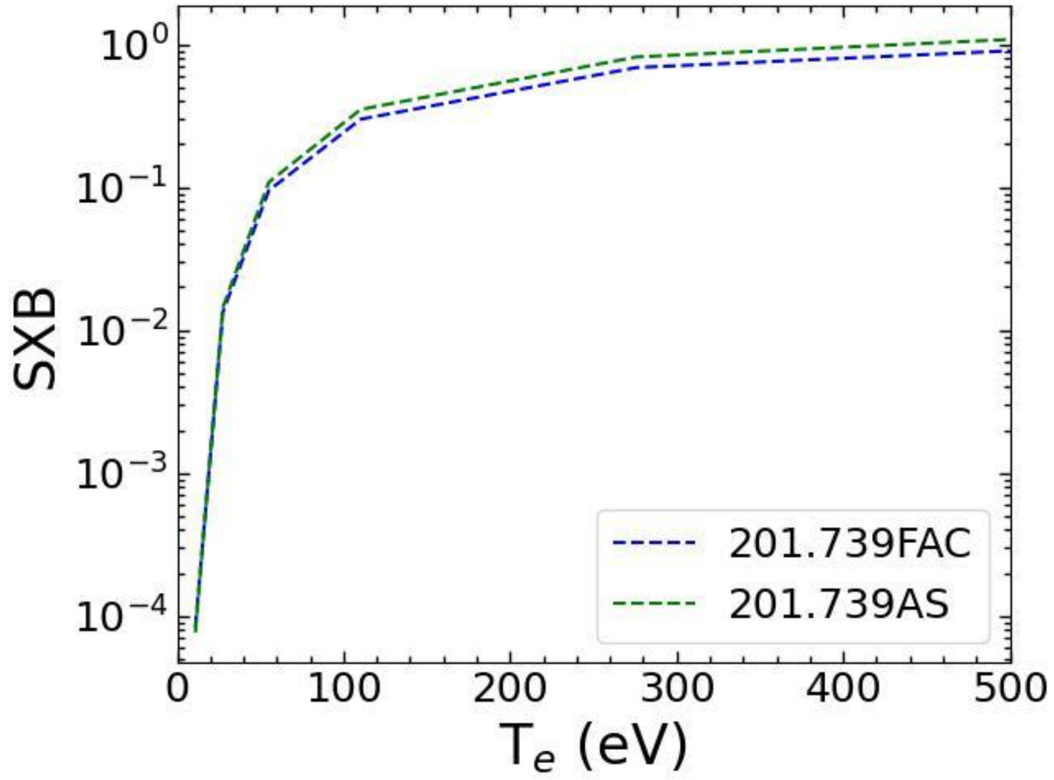

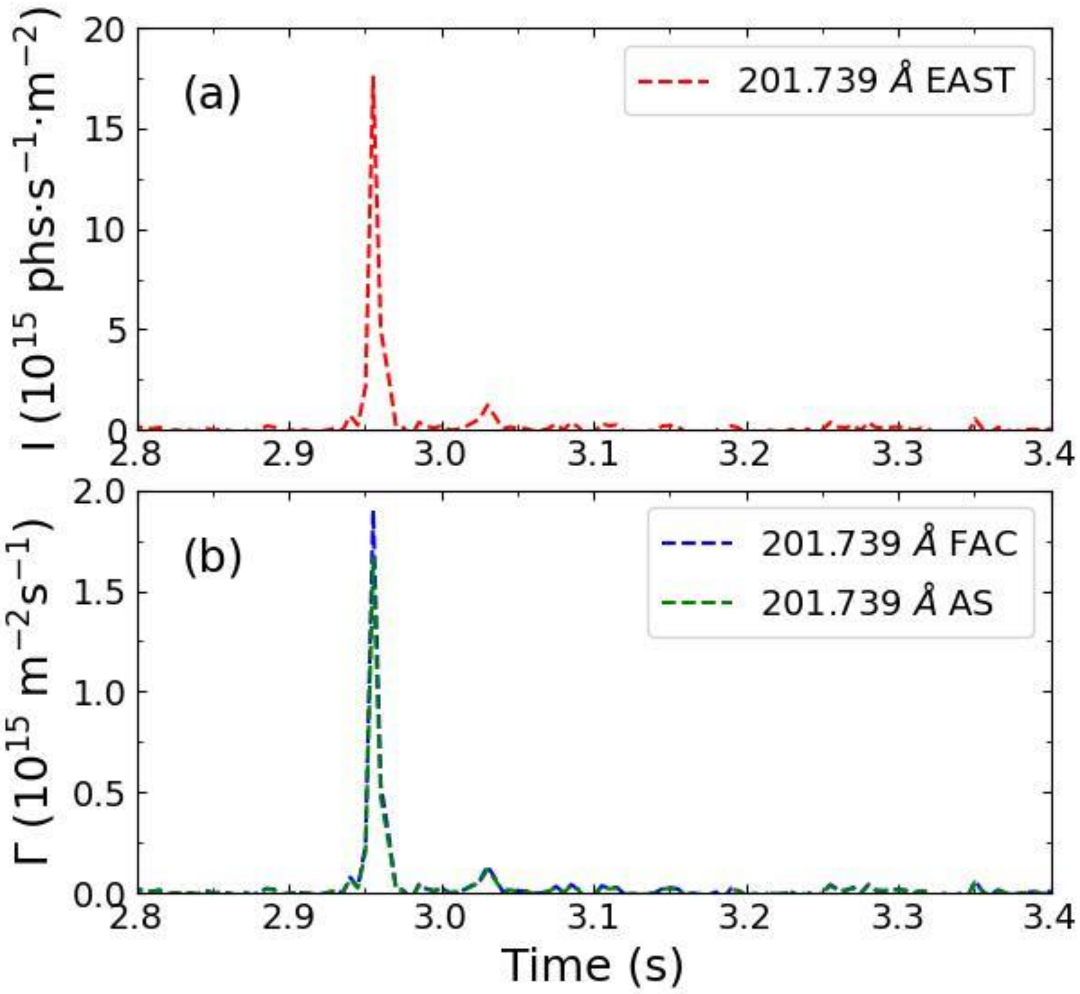

- SXB (T_e) at a $n_e = 1 \times 10^{14}$ cm^{-3}
- Line: W^{7+} at 201.739 Å

(a) Line intensity observed in EAST #113762

(b) W^{7+} influx evaluated from line 201.739 Å at T_e=27.6eV

Outline

ASIPP

- Background & Motivation
- Tungsten spectroscopic diagnostics
- Tungsten line identification and density profiles
- Tungsten influx evaluation: S/XB calculation
- Summary & Future work

Summary & future work

ASIPP

- Set of fast-time-response EUV spectrometers and space-resolved EUV spectrometers have been developed in EAST tokamak to investigate the W spectra composition and W ion distribution respectively.
- Vertical intensity profiles of W^{42+}-W^{45+} are used to calculate the ion density profiles
- Totally 249 W lines observed and well identified in EUV range, in which 83 lines from W^{22+}-W^{45+} ions, **107 lines from W^{4+}- W^{8+} at 160-480 Å, 59 lines are newly discovered** including several isolated W lines with strong intensity.
- Preliminary calculation of S/XB has been finished and applied to evaluate the W ion influx.
- More precisely calculation of level population with CRM including full levels and many metastables is being performed.

Future plan on VIS spectroscopy

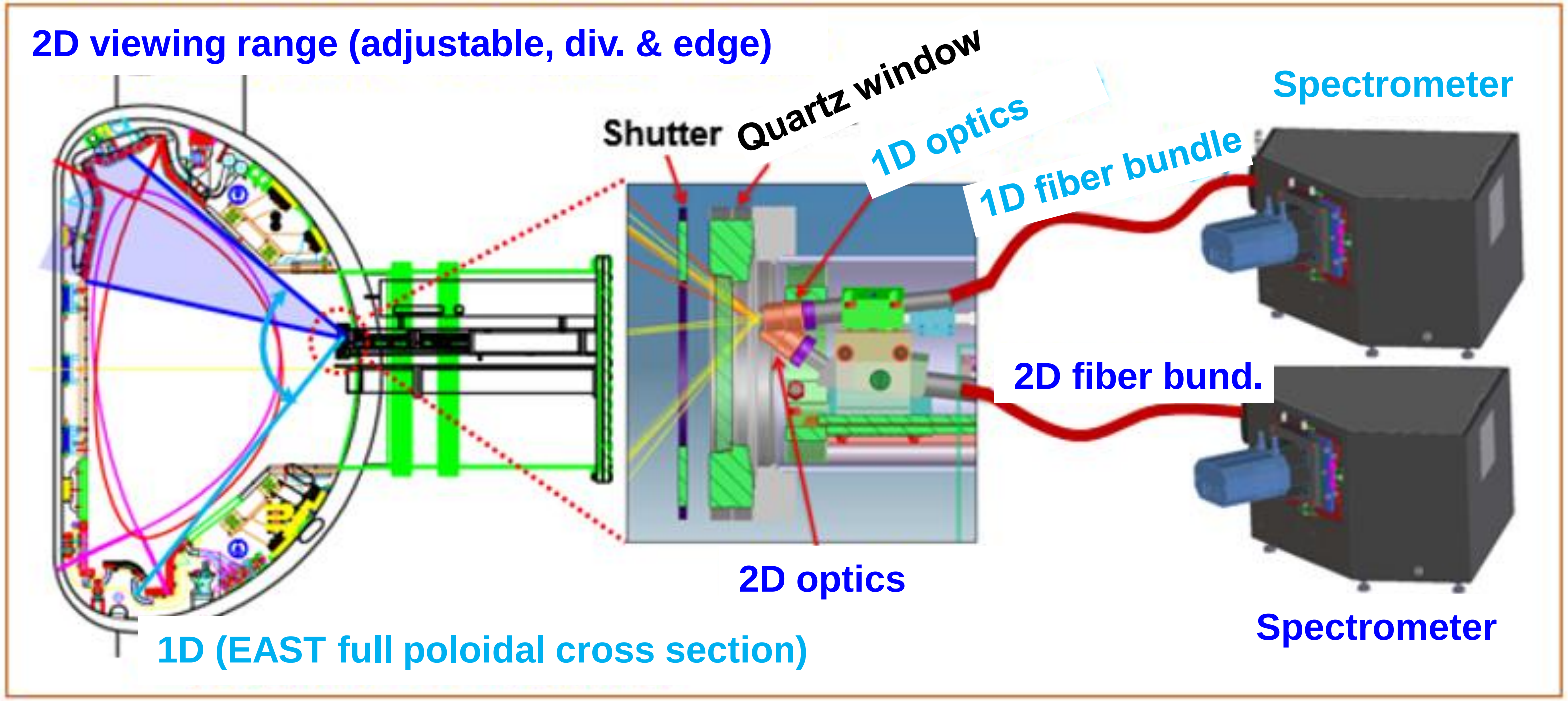

- Endoscopic optical design
- Two optics
  - 2D imaging (Div. & edge)
  - 1D large viewing range (EAST full cross section)
- Main components
  - Shutter, quartz window
  - Optics, fiber bundles
  - Spectrometer, detector

- **Endoscopic optics**
  - 2D at upper divertor: 85 x 38 cm^2 (poloidal x toroidal, remote controllable)
  - 1D full radial profile: ΔZ=145 cm
- **Fiber bundles**
  - 2D: 11 x 10 (50/62.5 μm)
  - 1D: 60 (115/125μm)
- **Quartz window for viewing port**

- **Shutter with supersonic motor**
- **Spectrometers (MK-300)**
  - Entrance slit: 0.01-4.0mm
  - Gratings: 2400, 1200, 300 g/mm
- **Detector: Andor Marana CMOS**
  - 2048 x 2048 pixel,
  - 11μm, 22.53 x 22.53 mm

Development & Commissioning

- System design: from Sep. 2020
- Manufacture & delivery: April. 2022
- Installation: Oct.12 - Nov. 7, 2022
- Optical alignment: mid. of Sep. 2023
- 2nd Calibration: end of Sep. 2023

A.L. Hu *43rd ITPA-DG* 2023

Future plan on VIS spectroscopy

EAST Divertor plates

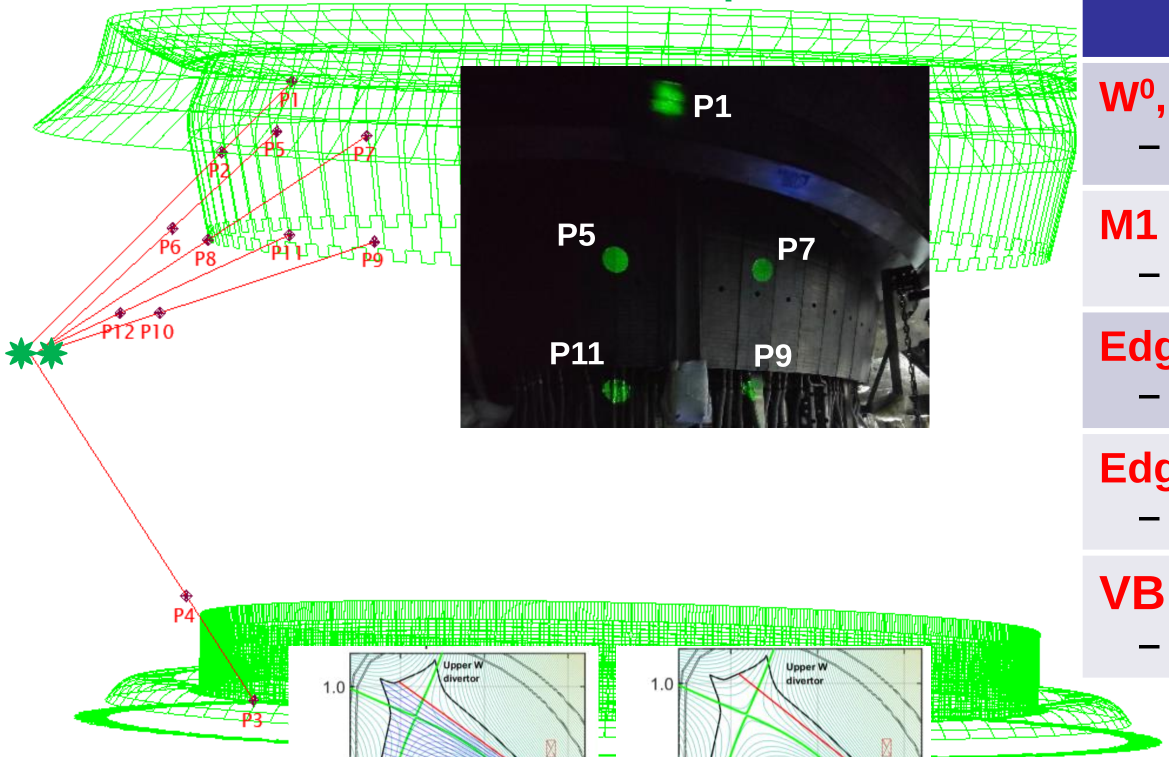

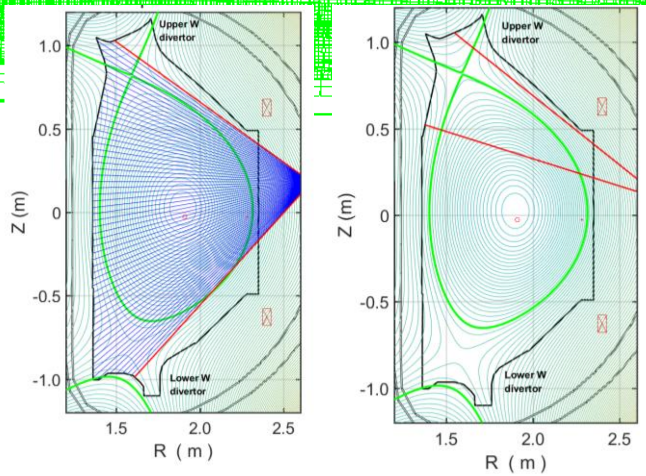

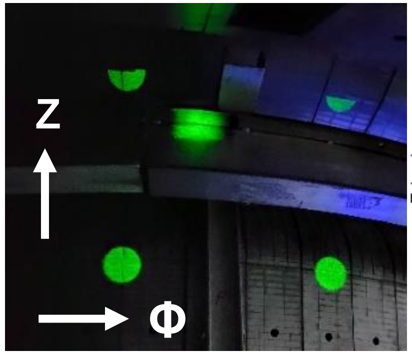

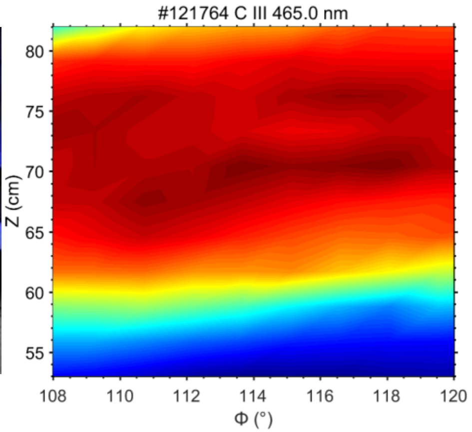

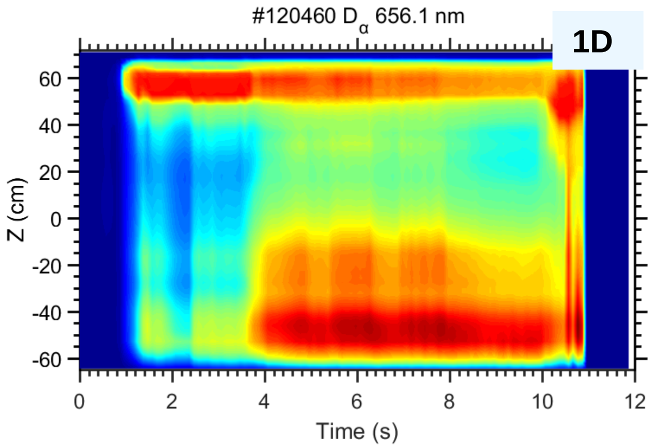

Tungsten & Impurity	Deuterium
W^0, W^0, C^{2+} source − 1D & 2D, 1200/2400 g/mm	**D_β/D_γ … during detachment** − 1D & 2D,1200 g/mm
M1 transition from W^{7+}-W^{28+} − 1D, 1200 g/mm	**D_2 Fulcher-α band** − 2D,1200/2400 g/mm
Edge Impurity survey at 300-800nm − 1D & 2D, 300 g/mm	**Verification of div. conf.** （Snowflake, Fish tail） − 2D, 300/1200 g/mm
Edge impurity flow from Doppler shift − 2D, 2400 g/mm	**DB, DW molecular ?**
VB, Z_{eff} profile → EUV calibration − 1D, 1200 g/mm	

Thanks for your attention!

ASIPP

Specifics of M1 lines

ASIPP

◆ **Allowed transition**
- ➢ **Electrical dipole (E1: Δl=±1)**

◆ **Forbidden transition**
- ➢ **Magnetic dipole (M1: Δn=0 and Δl=0)**
- ➢ **Electric quadrupole (E2: Δl=0, ±2)**

Specific character of M1 lines

- **The wavelength of M1 transition is much longer than E1 transition**
  - λ becomes constant in visible range for the Ti-like M1 transition for Z>50
    - Easy to observe: Doppler shift → ion temp.
- **Important for high Z impurities**
  - Transition probability, A, quickly increase with Z, e. g. $A \propto Z^{10}$
  - Intensity largely increases for high-Z ions
  - Intensity depend on electron density.

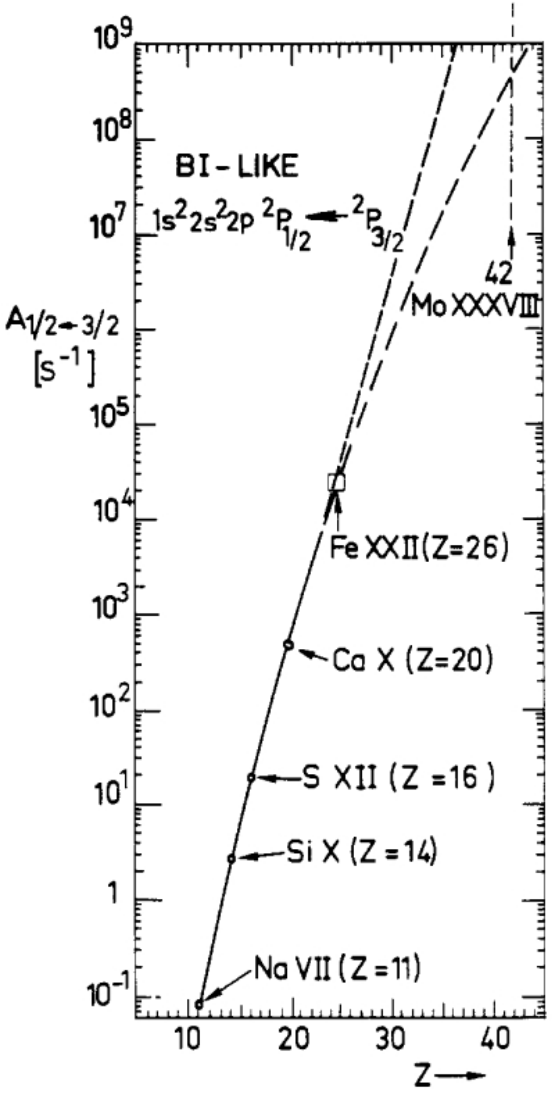

Transition rate of B-like M1 line ($1s^22s^22p\ ^2P_{3/2} \rightarrow ^2P_{1/2}$)

Z	Ion	A [s^{-1}]
11	NaVII	8×10^{-2}
16	SXII	2×10^{1}
20	CaX	5×10^{2}
26	FeXXII	2×10^{4}
42	MoXXXVIII	10^{9}~10^{10}

Comparable to E1

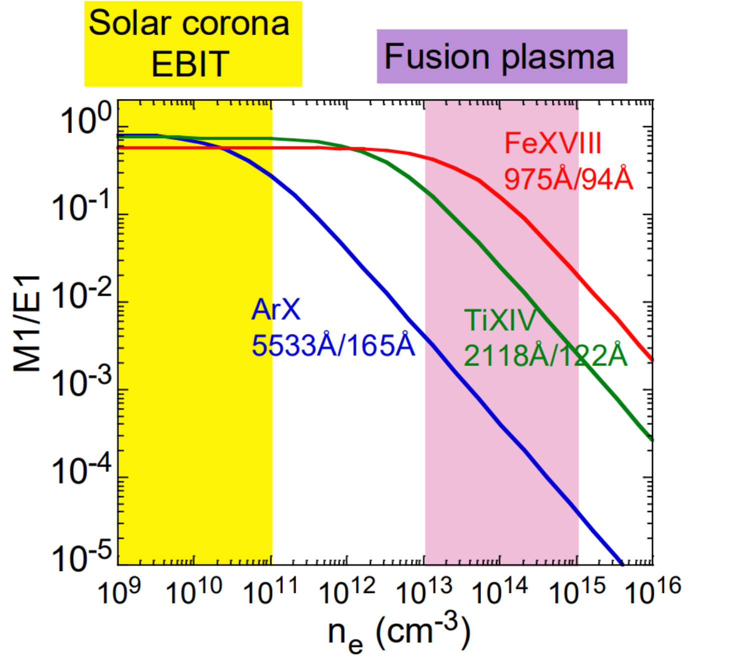

H. W. Drawin, Phys. Scr. 24 (1981) S. Morita, 6th APCPP: AAPPS-DPP (2022)

Observation of M1 lines

Visible M1 lines from W^{7+} - W^{28+} ions observed in EBIT and LHD

TABLE I. Visible wavelength of tungsten forbidden transition, in nm.

Ions	CoBIT	E_C (eV)	SH-HtscEBIT	E_S (eV)	MCF device
28	365.25, 393.06 [1]	940	220.97, 365.36, 393.20 [10]		344.48 [11]
27			377.743 [10]		337.73 [11]
26	389.41, 464.68, 501.99, 389.41, 464.68, 501.99 [1]	825	263.26, 291.89, 333.75, 335.76, 389.43, [10]	1200	389.39, 333.70, 335.73 [11]
25	383.99, 400.88, 406.92, 421.28, 451.15, 467.59, 469.21, 493.62 [1]	775	493.84, 587.63, 226.97 [10]		
24	364.58, 374.34, 375.70, 379.64, 386.23, 389.89, 392.62, 406.49, 408.58, 409.97, 419.35, 425.17, 447.36, 467.80, 468.22, 471.18 [1]	725			
23	366.48, 375.18, 388.27, 409.44, 432.32, 432.66, 437.90, 438.30, 441.52, 449.46, 459.25 [1]	675			
22	384.32, 446.95 [1]	630			
21	382.21, 415.83, 424.17, 442.69, 444.58, 450.70, 451.17, 459.99, 463.50, 468.39 [1]	585			
20	388.25, 402.91, 406.62, 422.05, 425.27, 433.14, 435.82, 438.02, 448.47, 462.40 [1]	535			
19	402.52, 433.89, 441.06, 456.43, 474.49 [1]	495			
18	375.90, 376.85, 396.83, 401.22, 419.68, 434.01 [1]	455			
17	373.69, 391.93 [1]	415			
16	472.39 [1]	380			
15	374.39, 378.14, 384.15, 384.76, 412.17, 414.29, 420.52, 424.45, 426.47, 428.43, 436.92, 450.23 [1]	340			
14	527.27, 388.19, 399.81, 496.55, 535.9,	320			
	549.33, 540.53, 451.68, 483.26, 480.09	320	549.3, 540.5, 451.65, 483.26, 480.08 [2]		
13	457.26, 459.08, 472.68, 457.26, 459.08,	280	462.64, 549.95, 432.24, 409.52,	300	
	472.68 [1]	280	546.23, 527.74, 486.63, 717.77 [9]	300	
12	401.38, 451.68 [1]	250	527.74, 388.16, 399.78, 496.52, 535.87, 660.3,	232	
11	388.19, 399.81, 446.04, 452.77, 454.64, 466.48 [1]	225	527.61 [5]	220	
10			419.75, 446.83, 452.40, 468.22, 527.44 [6]	170.5	
9	409.66, 438.68, 481.55, 533.20, 608.41	150	431.73, 447.13, 477.25, 470.56,		
	409.66, 438.68, 481.55, 533.20, 608.41 [8]	150	611.13, 645.48		
8	387.15, 405.73, 431.78, 447.14, 477.29,	130	431.73, 447.13, 477.25, 470.56,	127.1	
	570.52, 611.17 [1,8]	130	611.13, 645.48 [7]		
7	574.47 [3]	115	574.49 [4]	90	

Intensity profiles M1 line in LHD

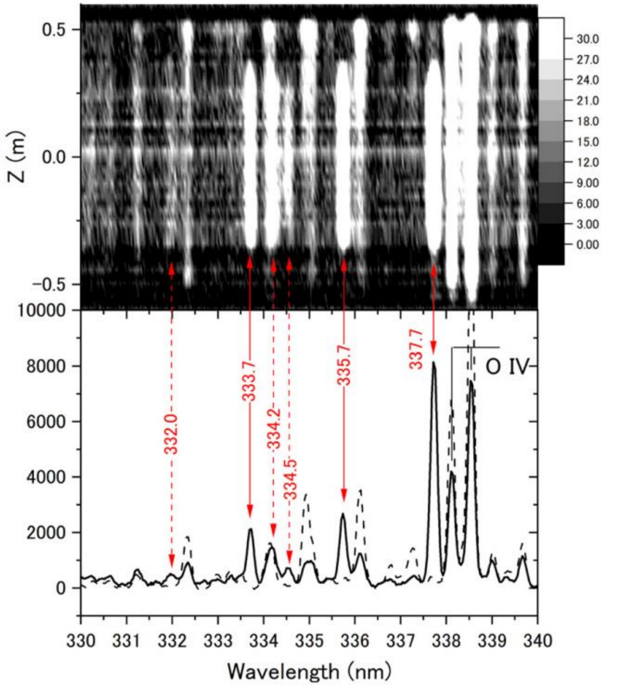

[1] Komatsu et al. Physica Scripta, T156, 2012.
[2] Kobayashi et al. Physical Review A, 92, 2015.
[3] Mita et al. *Atoms*, 5, 2017.
[4] Lu, Q et al. Physical Review A, 99, 2019.
[5] Lu, Q i et al. Journal of Quantitative Spectroscopy and Radiative Transfer, 279, 2022.
[6] Lu, Q i et al. Journal of Quantitative Spectroscopy and Radiative Transfer, 262, 2021.
[7] Lu, Q et al. Physical Review A, 103, 2021.
[8] Priti et al. Physical Review A, 102, 2020.
[9] Zhao, Z. Z. et al. Journal of Physics B, 48, 2015.
[10] Qiu, M. L. et al. Journal of Physics B, 48, 2015.
[11] Kato, D. et al. Physica Scripta, T156, 2013.

ASIPP

EAST	Capability	Diagnostic
Divertor	Upper & lower div. W source – **W^0 (4009Å)**	**Space-resolved VIS**
	Upper div. W source (**2D**) – **W^0** (4009Å, 4295Å, 5053Å) – **W^{1+}** (4218Å, 4348Å)	**Space-resolved VIS (2D)**
SOL (ρ=1.0-1.05)	W influx (**W^{3+}-W^{6+}: 500-1500Å**)	**VUV survey**
	W influx (**W^{3+}-W^{6+}: 200-500Å**)	**EUV survey**
Pedestal / edge	W influx & density – **W^{7+}-W^{20+}: 150-260Å**	**EUV survey**
Bulk plasma (ρ≤0.7)	W density profile – **W^{24+}-W^{45+}: 15-140Å**	**Space-resolved EUV**